ABSTRACT

ATKINS, BENJAMIN COVINGTON. Characterizing the Effect of pH and Molecular Structure on the Reactions of Catechol and Hydroquinone with Birnessite. (Under the direction of Dr. Hui Li)

The mechanisms underlying the formation and stability of soil organic matter (SOM) remain largely unclear and are dependent on a host of environmental and chemical factors. Yet, as the role of soils in carbon storage and cycling is increasingly recognized, this information that is crucial. The polyphenol theory is one commonly accepted pathway for the formation of SOM, and has been shown to occur biotically or abiotically. Birnessite is a layered Mn-oxide that is ubiquitous in soils and is capable of promoting polymerization reactions of polyphenols. Previous research has not fully elucidated the effect of pH and molecular structure of the parent materials on such reactions, nor have they characterized the degradation products formed. To contribute to this understanding, we performed batch experiments at three environmentally relevant pH conditions to examine the reaction of birnessite with the polyphenols catechol and hydroquinone. Spectroscopic analyses were employed to glean information on the formation of humic-like polymers and simple degradation products. These analyses complemented measurements of dissolved Mn and organic carbon which provide insight into the reaction progress under varying conditions. Catechol reduced Mn and dissolved the mineral more than hydroquinone, and this dissolution was greater at low pH. Correspondingly, more carbon was lost from the system during catechol reactions compared to hydroquinone. Spectral data supports the concomitant formation of humic-like polymers and aliphatic degradation products which vary according to pH and compound used. Overall, the results show a clear impact of pH and molecular structure on the interaction of polyphenols with birnessite.

Characterizing the Effect of pH and Molecular Structure on the Reactions of Catechol and Hydroquinone with Birnessite

by

Benjamin Covington Atkins

A thesis submitted to the Graduate Faculty of North Carolina State University
in partial fulfillment of the requirements for the degree of
Master of Science

Soil Science

Raleigh, North Carolina
2024

APPROVED BY:

_____	_____
Hui Li Committee Chair	Owen Duckworth
_____	
Elon Ison	

BIOGRAPHY

Ben Atkins was born in Brandon, Florida and is the son of Michael and Janice Atkins. He grew up on a small family farm in rural Lunenburg County, Virginia. This upbringing allowed him to spend a great deal of time outdoors – often playing sports or exploring the woods. Ben has fond memories of days spent working with his family on various jobs to be done. This background instilled a hardworking nature and love for the environment.

Ben enrolled at Virginia Tech in 2017, pursuing a bachelor's degree in Environmental Science. Coursework in soil science and chemistry allowed him to realize his interests in each of these areas. His knowledge of soil science blossomed as participation on the Virginia Tech Soil Judging Team provided hands-on experience and deep understanding of soil formation. This experience culminated in a first-place finish as an individual and team at the National Collegiate Soil Judging Competition in 2022, and the opportunity to represent the United States at the International Soil Judging Competition in 2022. Earning a minor in Chemistry allowed him to deepen his knowledge of this subject and realize his interests in environmental organic chemistry. After taking one year off from school to work full-time at a soil consulting firm in Richmond, VA, Ben returned to Virginia Tech to graduate in spring 2022.

Ben began his master’s at North Carolina State University in fall 2022, and currently studies the reactions of manganese oxides with model organic compounds in the context of soil organic matter formation.

TABLE OF CONTENTS

LIST OF TABLES

LIST OF FIGURES

SECTION 1: INTRODUCTION

Soils are a critical component of the global carbon cycle. Global estimates suggest that 1500 billion tons of C is stored in soil (European Commission. Directorate General for the Environment., 2011), greater than the amount found in global vegetation and the atmosphere combined (Lehmann and Kleber, 2015). As climate change and population growth continues to occur, it is becoming increasingly important to properly manage the soil organic carbon pool and predict carbon fluxes from soils. Doing so requires a thorough understanding of the mechanisms that are involved in the formation and stabilization of soil organic matter (SOM).

Soil organic matter consists of a continuum of organic molecules added to the soil by plants and other soil dwelling organisms. Beyond natural sources, a host of anthropogenic sources also contribute organic compounds to the soil. These molecules are at various stages of decomposition, and may be able to react with each other and with soil minerals. Breakdown of these materials may result in conversion to carbon dioxide (CO_2) and release to the atmosphere or leaching to local surface and groundwaters. However, they may also become stabilized in the soil and remain for extended periods.

Stable organic molecules formed in soil are often termed ‘humic substances’. Presently, the definition of humic substances and mechanisms for their formation remains a point of contention. Generally, the term humic substances applies to molecules that have undergone a chemical transformation that has rendered them relatively less susceptible to metabolism. These molecules are expected to have a longer residence time in soil compared with more labile molecules including sugars and carbohydrates (Flaig et al., 1975; Stevenson, 1982). The term humification is used to describe the accumulation of humic substances in soil, and is usually accompanied by melanization.

In some cases, humic substances have been regarded as low molecular weight organic molecules that form supramolecular associations (Simpson et al., 2001). As such, they have been thought to include an array of naturally occurring organic molecules as a mixture of carbohydrates, lipids, proteins, partially degraded lignins, etc. (Burdon, 2001). It should be noted that environmental organic matter refers to both humic and non-humic substances (Hardie, 2008). Along these lines, Lehmann and Kleber pose a soil continuum model for humic substances, whereby organic matter additions to the soil are gradually being degraded until mineralization to CO_2 (Lehmann and Kleber, 2015). Mineral association and aggregation of organic molecules serve as the dominant routes for SOM stabilization in their view. In the soil continuum model, molecules are not expected to react with each other or with mineral components to form new molecules. This view stands to contrast the classical ideas of humic substance formation, which involve the in situ synthesis of macromolecules through polycondensation and polymerization reactions (Hayes and Swift, 2020). According to Gerke et al., in this classical view the stability of humic substances can arise through the presence of recalcitrant aromatic cores or reaction with mineral surfaces (Gerke, 2018). Though a consensus does not exist for how humic substances form, it is likely that the true path involves a combination of the various ideas presented.

Synthetic humification processes occur through both biotic and abiotic mechanisms, including but not limited to the Maillard reaction (Hardie, 2008) and the polyphenol pathway (Stevenson, 1982). The polyphenol theory suggests that the degradation of lignin or cellulose derived from plant materials serves as the starting point for synthesis of humic compounds. As lignin molecules are decomposed, phenylpropane units are formed. Subsequent oxidation of side chains via decarboxylation and demethylation allows for the formation of low molecular weight

aromatic acids and aldehydes. Further oxidation and introduction of hydroxyl groups leads to the formation of reactive polyphenol compounds, which have multiple -OH functional groups attached to an aromatic ring. Fungi are instrumental in degrading lignin, but may have limited capacity to further degrade the resultant aromatic rings which serve as the structural units in the supramolecular structure of lignin (Stevenson, 1982). Aside from the breakdown of lignin, microorganisms have been shown to synthesize polyphenols, and this contribution can partially explain the presence of humic substances where there is no significant source of lignin (Stevenson, 1982). The pathways that have been previously proposed are not mutually exclusive, and some researchers have explored the idea of an integrated Maillard-polyphenol pathway in which these two reaction pathways may be intertwined in natural systems, both contributing to the formation of humic substances (Jokic et al., 2004).

Polyphenols occur naturally in various biological settings. As previously mentioned, these molecules, can be synthesized from aliphatic molecules by microorganisms. Additionally, these polyphenols are naturally found in the flesh of plants and fruits. Here, they are known to serve as antioxidants capable of reacting with free radical species and complexing metals (Choe, 2020). The hydroxyl moieties present in these molecules are readily able to donate a hydrogen atom to radical species to form resonance stabilized phenoxyl/semiquinone radicals that are less reactive and may then couple to form dimers or partake in metal chelation (Choe, 2020). Polyphenol molecules are important in the production of melanin in plants and animals. Catechol-melanin, a brown insoluble pigment is thought to form via oxidation of catechol by polyphenol oxidase and subsequent coupling of semiquinone species via C-C or C-O linkages (Swan, 1974).

The polyphenols formed in soil are susceptible to enzymatic degradation by microorganisms or reaction with mineral phases. In either case, the oxidation of these phenolic compounds results in the formation of highly reactive quinones and free radical species. Enzymes such as tyrosinase and polyphenol oxidase have been shown to be involved in the conversion of polyphenols into quinones (Naidja et al., 1998; Stevenson, 1982). In an iterative process, the interaction of these quinone molecules results in the formation of polymerized species of variable molecular weight and composition. In reference to this coupling process, Ito et al. note that the reactions are so complex that general conclusions cannot be drawn (Ito et al., 2020). Thus, individual mechanistic studies are necessary to examine different aspects of the reactions. The collective findings of these studies will provide a more clear picture of the processes that occur.

Manganese oxides (Mn-oxides) have been shown to catalyze abiotic humification reactions (Hardie, 2008; Liu et al., 2011; Shindo and Huang, 1982). Many previous studies that have examined the contribution of Mn-oxides in these reactions have focused on birnessite because it is one of the most common forms of Mn-oxide identified in the soil environment (Di Leo et al., 2012). Composed of layers of edge-sharing MnO octahedra, birnessite is characterized by a high specific surface area and a negatively charged surface (point of zero charge ~ 2) under most common soil pH conditions (Matocha et al., 2001). The layer charge in birnessite is balanced by an interlayer of hydrated cations. The identity of the cation occupying the interlayer varies, but is most commonly Na^+, K^+, Ca^{2+}, or H^+. Natural samples may have a combination of cations, whereas synthetic birnessite minerals will vary according to the method used during synthesis (Potter and Rossman, 1979). Birnessite is classified into one of two groups based on the symmetry of the octahedral layer which affects the structure of the crystal lattice. In triclinic

birnessite, rows of Mn(III) and Mn(IV) octahedra alternate, with no vacancies within the layer. Conversely, hexagonal birnessite layers are predominantly composed of Mn(IV) octahedra with asymmetric substitution of Mn(III) octahedra. This asymmetry creates vacancies within the layer that can be occupied by interlayer cations (Li et al., 2024). Synthesis in acidic media typically produces hexagonal birnessite, whereas triclinic birnessites are produced under alkaline conditions (Li et al., 2024).

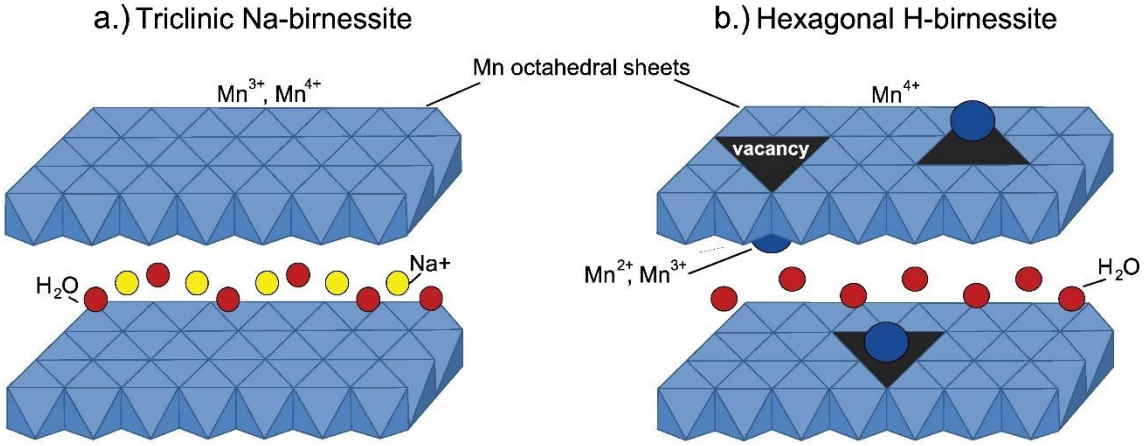

Figure 1.1: Octahedral layer structure of triclinic and hexagonal birnessite (Ling et al., 2017).

The electrode potential of birnessite (E^o = +1.29) allows for efficient oxidation of organic molecules such as the polyphenols previously discussed (Stone, 1987). However, the impact of solution pH and molecular structure of the starting compounds on such reactions remains unresolved. In this study, we use two simple polyphenol isomers, catechol and hydroquinone, to serve as model organic compounds to study these reactions under varying pH conditions and consider how the position of -OH functional groups on the aromatic ring affects reactivity. Catechol (pK_{a1} = 9.3, pK_{a2} = 13.0) and hydroquinone (pK_{a1} = 9.9, pK_{a2} = 11.6) are mostly protonated in aqueous solution under the common environmental pH values of soils (Enguita and Leitão, 2013; Schweigert et al., 2001). It should be noted that although catechol and hydroquinone may occur in the soil environment, they also share the same reactive functional

groups that are present in larger SOM molecules. Therefore, the reactivity of these compounds will shed light on how larger compounds may also react, given that a portion of the structure is comprised of hydroxyl moieties attached to an aromatic ring in an ortho or para conformation.

Though relevance to SOM formation and carbon cycling is the focus of the current study, the capacity of Mn-oxides to degrade organic compounds also has applications in wastewater and soil remediation. The reactivity of Mn-oxides may be useful for removing recalcitrant trace organic compounds in wastewater (Remucal and Ginder-Vogel, 2014). Studying reactions of dissolved organic matter (DOM) in wastewater with Mn-oxides, Trainer et al. found that the resulting aqueous DOM after reaction was less aromatic and lower in molecular weight (Trainer et al., 2021). An array of xenobiotics which have aromatic rings may undergo hydroxylation during the degradation process, resulting in the presence of the reactive functional groups that we aim to study. Hydroquinone has been identified as a major metabolite of benzene, and catechols are known to be intermediates in the degradation of pesticides. Many other examples exist which provide evidence for the occurrence of catechol and hydroquinone in the environment, each of which carry concerns of carcinogenicity (Enguita and Leitão, 2013; Schweigert et al., 2001).

Proposed Mechanism and Rate Laws

Catechol/hydroquinone can undergo a redox reaction with birnessite, where birnessite acts as a Lewis acid by accepting electrons from the organic molecule. The proposed reaction mechanism for the reaction of catechol with birnessite is as follows (Matocha et al., 2001):

1. Formation of a precursor surface complex:

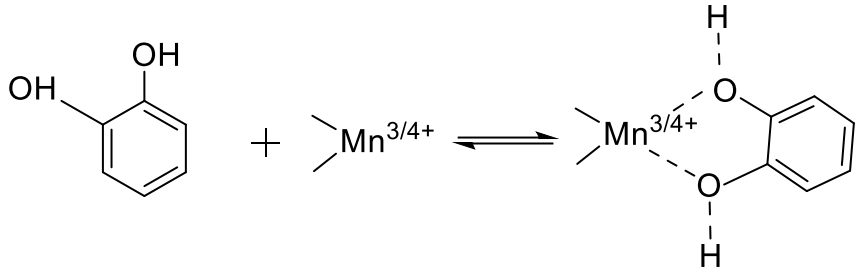

2. Electron transfer within the surface complex:

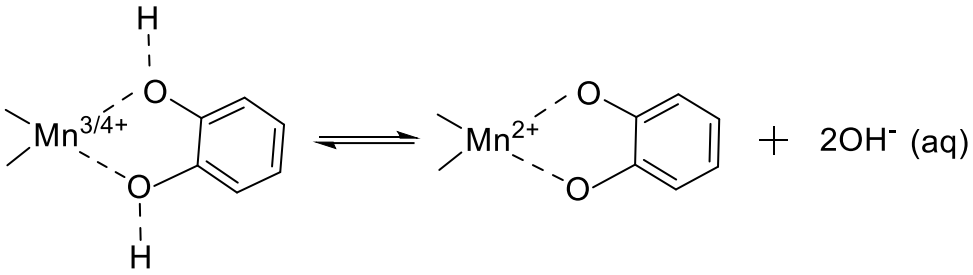

3. Product Release:

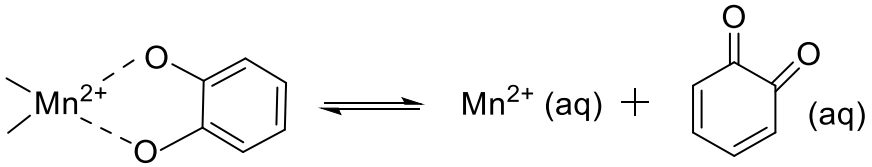

In the above reaction scheme, catechol forms a bidentate surface complex with a Mn atom located at the surface of the birnessite mineral. As shown, the surface complex is bidentate, mononuclear, however the formation of a bidentate, binuclear complex may also occur (Di Leo et al., 2012; Matocha et al., 2001). Two electrons are transferred to the Mn atom, resulting in the formation of Mn^{2+} within the crystal structure and two hydroxyls released to solution. In the final step Mn^{2+} is released to solution along with the o-benzoquinone product. Note that this may involve a release of a Mn-catecholate complex into solution which is later subject to degradation (Colarieti et al., 2006). In the event catechol binds to a structural Mn^{3+} atom, a single electron transfer is expected to occur, with the semiquinone product being formed instead of benzoquinone.

The proposed reaction mechanism for hydroquinone is as follows (Liu et al., 2011):

1. Formation of a precursor surface complex:

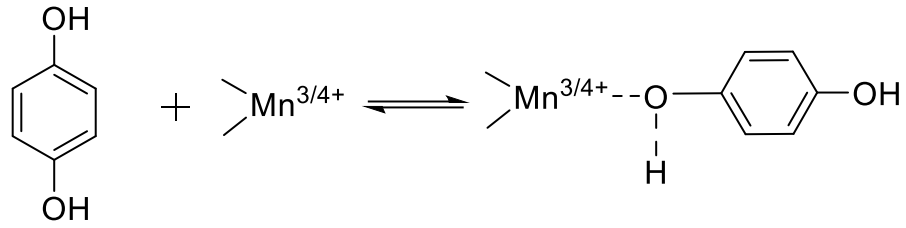

2. Electron transfer within the surface complex:

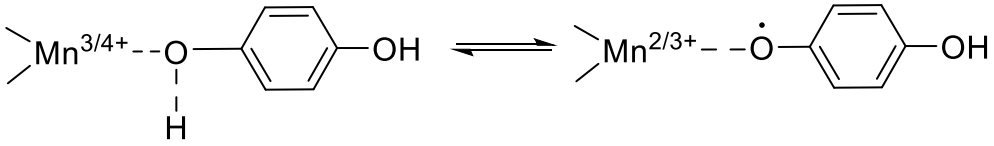

3. Product release:

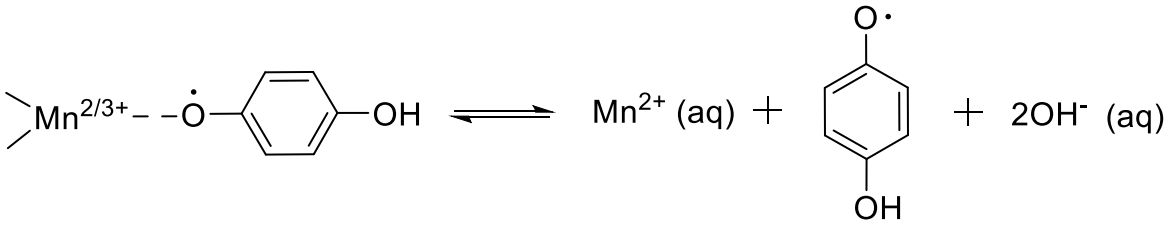

Hydroquinone is not able to form a bidentate surface complex due to the position of hydroxyl groups. Instead, a monodentate surface complex ensues with a single electron transfer, as shown in the above mechanism (Liu et al., 2011). The released semiquinone radical, although resonance stabilized, is expected to readily undergo coupling reactions upon interaction with other semiquinones. The semiquinone radical is also able to form a surface complex and become further oxidized via the same steps shown above to form p-benzoquinone. Alternatively, p-benzoquinone can form as a result of the loss of a proton by the semiquinone molecule and configurational transition. Release of p-benzoquinone can be accompanied by ring cleavage and the formation of carboxylic acid products (Liu et al., 2011).

The initial rate law for the catechol reaction, expressed in terms of the change in dissolved Mn as a function of time, is as follows:

$$\frac{d[Mn^{2+}]}{dt} = k[CAT][SA]$$

where k= 4 (± 0.5) × 10^{-3} L m^{-2} s^{-1},

[CAT] = concentration of catechol (M)

[SA] = total surface area of birnessite based on mineral loading (Matocha et al., 2001)

In this case, the rate of Mn^{2+} formation in the initial stages of the experiment was not found to be dependent on pH. The second order reaction was found to be first order with respect to the initial catechol concentration and total surface area of birnessite available for reaction to occur.

Studying the reaction of feitknechtite, a Mn(III) oxyhydroxide, with hydroquinone, Stone and Morgan devised the following rate law:

$$\frac{d[Mn^{2+}]}{dt} = k[HYD][SA][H^{+}]^{0.46}$$

where k = 1 $(L/mol)^{0.46}(L/m^2)(1/s)$,

[HYD] = concentration of hydroquinone (M), and

[SA] = total surface area of Mn-oxide based on mineral loading (Stone and Morgan, 1984a)

Here, pH was found to impact the initial rate of Mn-oxide dissolution, with higher pH resulting in less Mn^{2+} formed. Otherwise, the reaction was found to be first order with respect to the hydroquinone concentration and the surface area of the Mn-oxide.

Description of Reaction Products

A number of products have been identified and/or hypothesized to form as a result of the redox reaction. The general consensus appears to be that the reaction is capable of forming a

mixture of humic-like polymers, aliphatic fragments, and carbon dioxide (Chang Chien et al., 2009; Liu et al., 2011). Multiple researchers have interpreted the development of a brown solution color to be indicative of the formation of polymeric species that are comparable to natural humic substances (Shindo and Huang, 1982; Stone, 1987; Wang and Huang, 1992). Upon reaction with birnessite, these products are likely formed via the coupling of semiquinone or phenoxy radicals (Figure 1.2) (Johnson et al., 2015; Naidja et al., 1998).

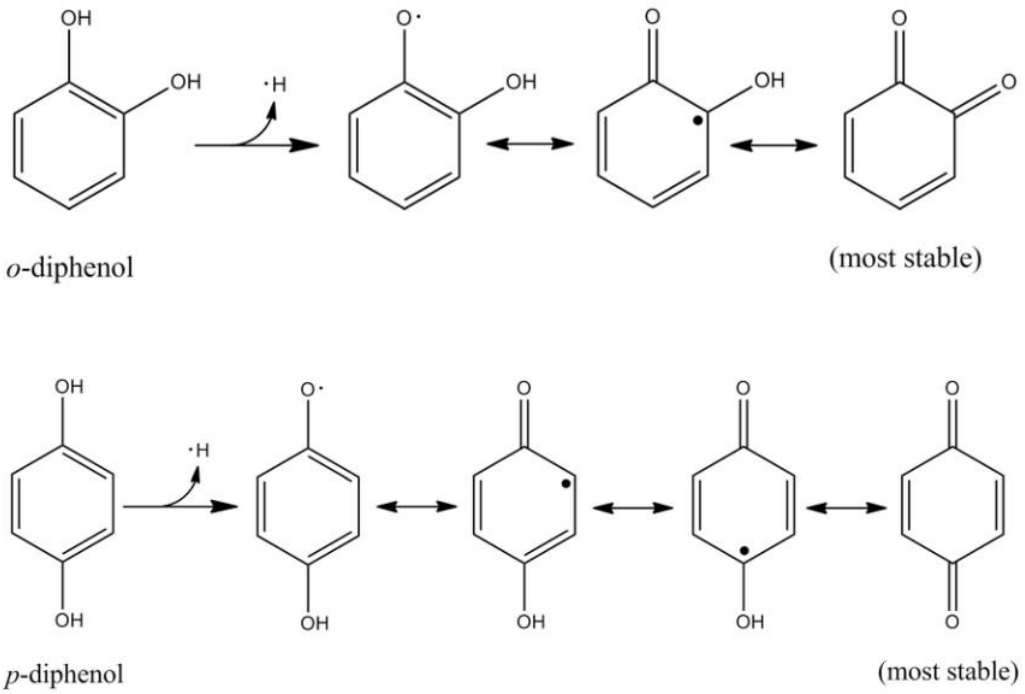

(Choe, 2020)

Figure 1.2: Resonance structures for catechol (o-diphenol) and hydroquinone (p-diphenol) radicals

No single product is expected to be produced since the coupling can proceed by any combination of monomers/dimers/oligomers. However, the formation of such polymeric substances does not necessitate the presence of radicals. Figure 1.3 below shows potential

mechanisms for the combination of benzoquinone molecules with diphenols still remaining in solution.

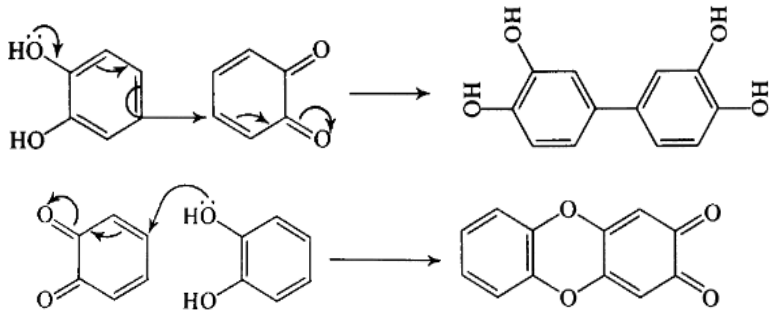

(Swan, 1974)

Figure 1.3: Potential mechanism for the formation of dimers with C-C or C-O linkages

Indirect evidence for polymerization is most easily attained using UV-vis spectroscopy. However, nuclear magnetic resonance, Fourier transform infrared spectroscopy, high performance liquid chromatography, and mass spectrometry have provided further evidence for the existence of these polymeric species, especially when used in conjunction (Naidja et al., 1998; Selvaraj et al., 2019; Šmejkalová et al., 2007; Wang and Huang, 1992). In studying the reaction of catechol with tyrosinase and birnessite, Naidja et al. identified the products shown in Figure 1.3 as probable reaction products, along with o-quinone, o-semiquinone, hydroxyquinone, and the hydroxyquinone radical (Naidja et al., 1998). The formation of hydroxyquinone shows that new hydroxyl groups can be introduced to the aromatic ring via oxidation by birnessite. Aside from the ability of hydroquinone and catechol to combine with each other in solution, it was found that birnessite promoted the addition of catechol to the structure of existing humic molecules through ester or ether linkages (Li et al., 2012). The ability of aromatic monomers to polymerize is important for the formation of mineral associations, especially considering that high molecular weight, UV-absorbing molecules with greater hydrophobicity were found to be

preferentially adsorbed to hexagonal birnessite compared with lower molecular weight molecules with more hydrophilic properties (Allard et al., 2017). Chang Chien et al. concluded that reaction under aerobic conditions would yield polymers with higher aliphaticity, whereas anaerobic conditions would yield polymers with higher aromaticity (Chang Chien et al., 2009).

Cleavage of the aromatic ring during the reaction of phenols with birnessite leads to the formation of carboxylic acids, including formate, acetate, and lactate (Jokic et al., 2004; Liu et al., 2011). Other carboxylic acids have been proposed to form via oxidation by ozone, including cis,cis-muconic acid, oxalic acid, maleic acid, and glyoxylic acid (Pillar-Little et al., 2015). Though ozone is a stronger oxidant ($E^o = 2.07$), the formation of some of these products is possible (Koppenol, 1982). Further oxidation of aliphatic fragments by birnessite can yield CO_2. Using ^{14}C labeled catechol, Majcher et al. found that up to ~2.2 mmol/L CO_2 formed from an initial C concentration of 13.8 mmol/L (Majcher et al., 2000).

Evidence that Mn-oxide promotes oxidative coupling reactions of phenols is well reported (Hardie, 2008; Jokic et al., 2004; Liu et al., 2011; Pal et al., 1994). Moreover, the observed formation of aliphatic fragments and CO_2 implies that Mn-oxide also acts to destabilize phenolic compounds (Allard et al., 2017; Majcher et al., 2000). The mechanism for the redox reaction involves surface complex formation, electron transfer, and release of oxidized organic and reduced Mn^{2+} species. Initial rates of dissolution of Mn-oxide as promoted by catechol or hydroquinone is thought to depend on the concentration of organic compound, total surface area of the mineral, and pH of the solution (Matocha et al., 2001; Stone and Morgan, 1984b). The mineral:organic molar ratio can have impacts on the progress of reaction and identity of products (Li et al., 2023). These reactions are relevant to questions of soil organic matter formation, carbon cycling, and wastewater/soil remediation. In this study, we have compared the reactions

of catechol and hydroquinone with birnessite under varying pH conditions. To date, a comparative study to detail the impacts of pH and molecular structure of reactants has not been performed. This study will address this knowledge gap by elucidating molecular scale interactions that will partially determine the cycling of soil carbon.

SECTION 2: MATERIALS AND METHODS

Batch Sorption Experiments

Birnessite (layer-structured δ-MnO_2) was prepared and characterized using X-ray diffraction (XRD) to determine the mineralogy. Details of the synthetic and characterization methods and results can be found in our previous paper (Li et al., 2023). The same batch was used in the current study.

Interactions between organic compounds and birnessite were studied via batch experimentation. Prior to each reaction, 0.1739 g of birnessite was suspended in 195 mL milli-Q water in a 250-mL Erlenmeyer flask. The suspension was stirred at a constant rate of 500 rpm. Additionally, a 40 mM stock solution of either catechol or hydroquinone was prepared by dissolving ~0.1762 g of each compound in about 40 mL milli-Q water. The actual stock solution volume was adjusted according to the exact mass of compound used. Individual stock solutions were prepared to limit autoxidation of the organic molecule prior to reaction. Sorption reactions were performed at pH 5, 7, and 8. These values were chosen to be representative of natural soil conditions since the majority of soil pH values will fall within this range. Prior to each reaction, the pH of the birnessite suspension and organic stock solution were adjusted to the target values (±0.05) using 1 M NaOH or 1 N HCl. The reactions commenced upon the addition of 5 mL of the organic stock solution to the birnessite suspension. The concentrations of the organic compound and birnessite at the onset of the reaction were 1.2 mM (88 mg C/L) and 8 mM, respectively. Throughout a 48-hour reaction period, 10-mL samples were taken at select time points. These samples were immediately filtered through 0.22µm polyethersulfone (PES) membrane filters (J.T. Baker). All filtrate and selected solid samples were frozen shortly after

and kept for further analyses. Select samples were re-analyzed after a period of 24 hours to verify that further reaction after filtration in the absence of a birnessite surface was negligible.

The stability of 1.2 mM catechol and hydroquinone in the absence of birnessite was tested at each pH condition. Birnessite control reactions tested the dissolution of MnO_2 in the absence of catechol or hydroquinone at each pH condition. To test the influence of O_2 in the reaction, a set of reactions were performed in a COY Laboratories anaerobic chamber with a N_2/H_2 atmosphere. Each combination of birnessite/organic compound/pH was duplicated in aerobic conditions and once in anaerobic conditions.

Degradation of Organic Compounds: Ultraviolet-Visible (UV-VIS) Spectroscopy

UV-vis spectroscopy was utilized to track the degradation of catechol/hydroquinone and gain information on the reaction products and degree of polymerization. Each sample was analyzed using a ThermoScientific Genesys 150 UV-Visible Spectrophotometer (Waltham, MA) in absorbance mode. Samples were tested using a continuous scan in the wavelength range of 200–800 nm with an interval of 2 nm. The λ_{max} of reference catechol, hydroquinone, and p-benzoquinone solutions were found at 275 nm, 288 nm, and 258 nm. Multiple studies (Hardie, 2008; Shindo and Huang, 1982; Stone and Morgan, 1984b; Wang and Huang, 1986) have suggested that an increase in absorbance across a range of wavelengths extending towards 800 nm is indicative of the darkening of the reaction solution as brown-colored humic-like polymers form. In particular, absorbance at 400 and 600 nm has been used to provide a semi-quantitative analysis of the yield of these polymer products.

Quantification of Dissolved Manganese(II)

The dissolved Mn^{2+} content was measured to provide an indication of the rate and extent of the reaction. One mL of each filtrate sample was preserved by 10-fold dilution in 0.1% HCl

and refrigeration at 4 °C until analysis. Select samples were further diluted 5-fold if found to be beyond the range of the calibration curve. Samples were analyzed using a PerkinElmer Optima 8000 optical emission spectrometer (Waltham, MA) using an excitation wavelength of 257.61 nm.

Dissolved Organic Carbon (DOC)

Given that a known quantity of organic compound was added at the inception of the reaction, tracking the amount of C remaining in the system as a function of time provides insight into the reaction progress and fate of the organic C during reaction. The initial concentration of organic compound, as measured by DOC, was 88 mg/L. Sample preservation involved 10-fold dilution of 1 mL of each filtrate sample with 0.1% HCl and storage at 4 °C. Analysis was performed using a Shimadzu TOC-L Total Carbon Analyzer (Kyoto, Japan).

Attenuated Total Reflectance Fourier Transform-Infrared Spectroscopy (ATR-FTIR)

Association of organic compounds with the mineral would be observed through the presence of new peaks, representing the association of major functional groups not present in the original birnessite spectrum. Solid-phase birnessite samples on the filters were freeze-dried and tested using FT-IR. Additionally, upon freeze-drying the filtrate samples, a solid-phase residue was formed which was the product of aggregation of the dissolved organic molecules present in the sample. All solid and freeze-dried organic residue samples were analyzed using an Agilent Technologies Cary 630 FTIR (Santa Clara, CA) from 4000 to 400 cm^{-1} in transmittance mode. Samples were placed directly onto a diamond crystal and pressed to maximize contact between the sample and the crystal. Unreacted birnessite provided a reference spectrum to compare

mineral samples, whereas catechol and hydroquinone served as reference spectra for the dissolved organic products.

Nuclear Magnetic Resonance (NMR) Spectroscopy

Nuclear magnetic resonance spectroscopy is used to identify organic compounds. Select samples were chosen and tested using ^{1}H – NMR, which detects hydrogen atoms within a sample and provides characteristic spectra based on their bonding environment. Samples were tested using a Bruker Avance III 700MHz spectrometer (Billerica, MA). A water suppression method was used with 64 scans and 4 dummy scans. Four mL of filtrate was freeze-dried and then re-dissolved in 650 μL of D_2O. The sample was then centrifuged at 8000 × g for 10 minutes to separate any undissolved particulates. Finally, 560 μL of the supernatant was transferred to an NMR tube for the analysis. The presence of dissolved Mn^{2+} in samples did not appear to interfere with spectra, and thus no steps were taken to precipitate and remove Mn^{2+}. Solutions of catechol and hydroquinone (1 mM) were tested for comparison. Contribution of organic molecules from the PES filter was tested by filtering three samples of milli-Q water adjusted to the experimental pH values 5, 7, and 8. Additionally, the solutions of 1 N HCl and 1 M NaOH used for pH adjustment were characterized via NMR.

Quantification of Solid-Phase Carbon

The concentration (weight %) of C in solid phase samples was quantified. Given that CO_2 evolution was not directly measured during these reactions, this measurement along with DOC has been used as a proxy to determine how much inorganic C may have been lost during the reaction. Freeze-dried solid phase samples (0.5–2 mg) were sealed in tin capsule pellets. These pellets were pyrolyzed by using an Elementar UNICUBE elemental analyzer to provide information on changes in C% within the first hour, at 5 hours, and at 48 hours.

SECTION 3: RESULTS AND DISCUSSION

3.1 **Change in dissolved organic carbon**

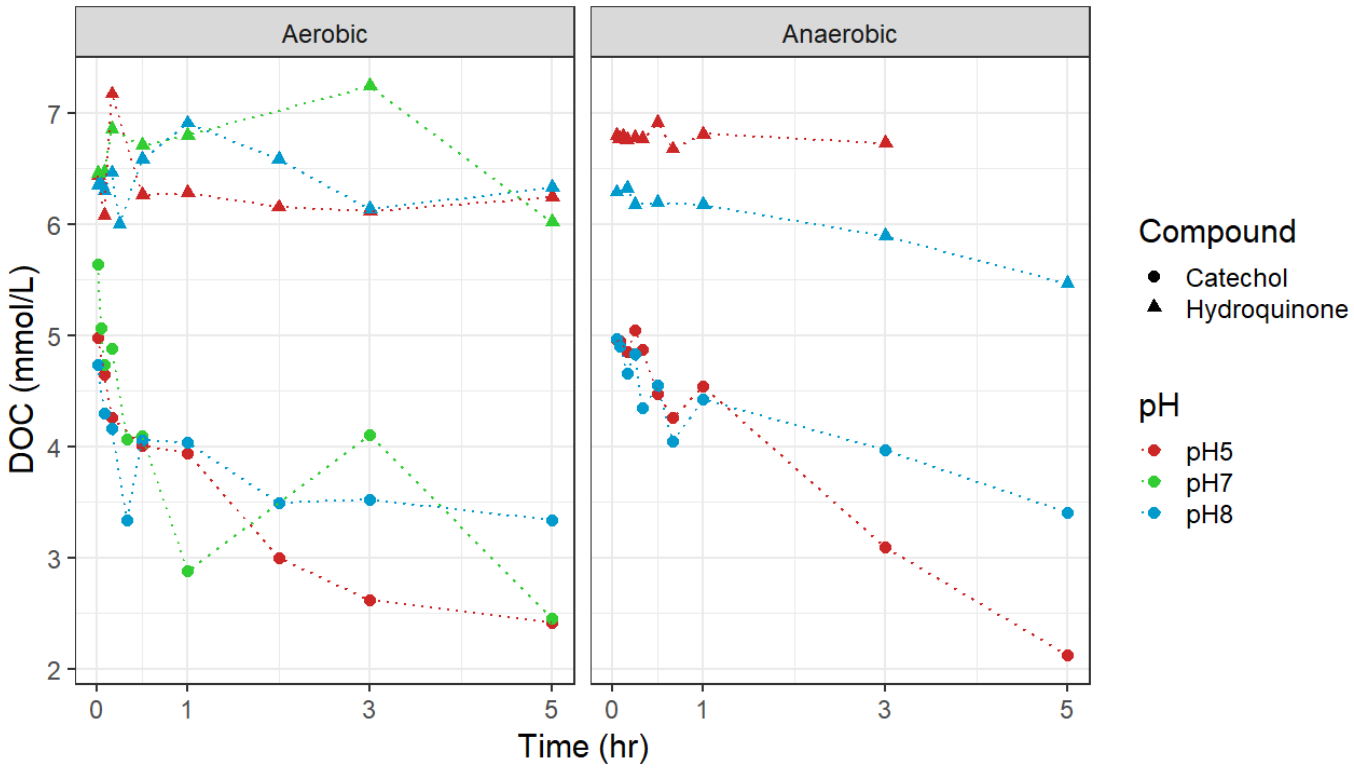

Figure 3.1. Temporal changes in DOC concentrations in supernatants after reacting with catechol and hydroquinone at different pH conditions.

Under aerobic and anaerobic conditions, dissolved organic carbon in solution decreased as the reaction progressed. (Figure 3.1). In general, there is a larger decrease in DOC derived from catechol than hydroquinone at all studied pH conditions. In addition, for catechol, more DOC is lost from solution as pH decreases from pH 8 to 5. The observed loss of organic carbon (OC) can be explained by sorption to the solid phase birnessite or oxidative decomposition into inorganic forms (e.g. CO_2). The pH dependency of the reactions may be relevant to the speciation of organic compounds and mineral surface charges. Due to high pKa values of catechol (9.3, 13.0) and hydroquinone (9.9, 11.6) (Enguita and Leitão, 2013; Schweigert et al., 2001), most of the catechol and hydroquinone molecules will be protonated. However, as pH

increases from 5 to 8, decreasing fractions of catechol and hydroquinone will be protonated and correspondingly increasing fractions of these organic compounds will be deprotonated. Singly coordinated oxygen atoms located at edge sites of birnessite minerals have been reported to have pKa values between 6 and 8 (Balgooyen et al., 2020; Wang et al., 2018; Zhang et al., 2022). Thus, a weaker electrostatic attraction and stronger electrostatic repulsion may occur at pH 8 that leads to less sorption at pH 8 than at lower pH conditions.

3.2 **Reductive dissolution of birnessite**

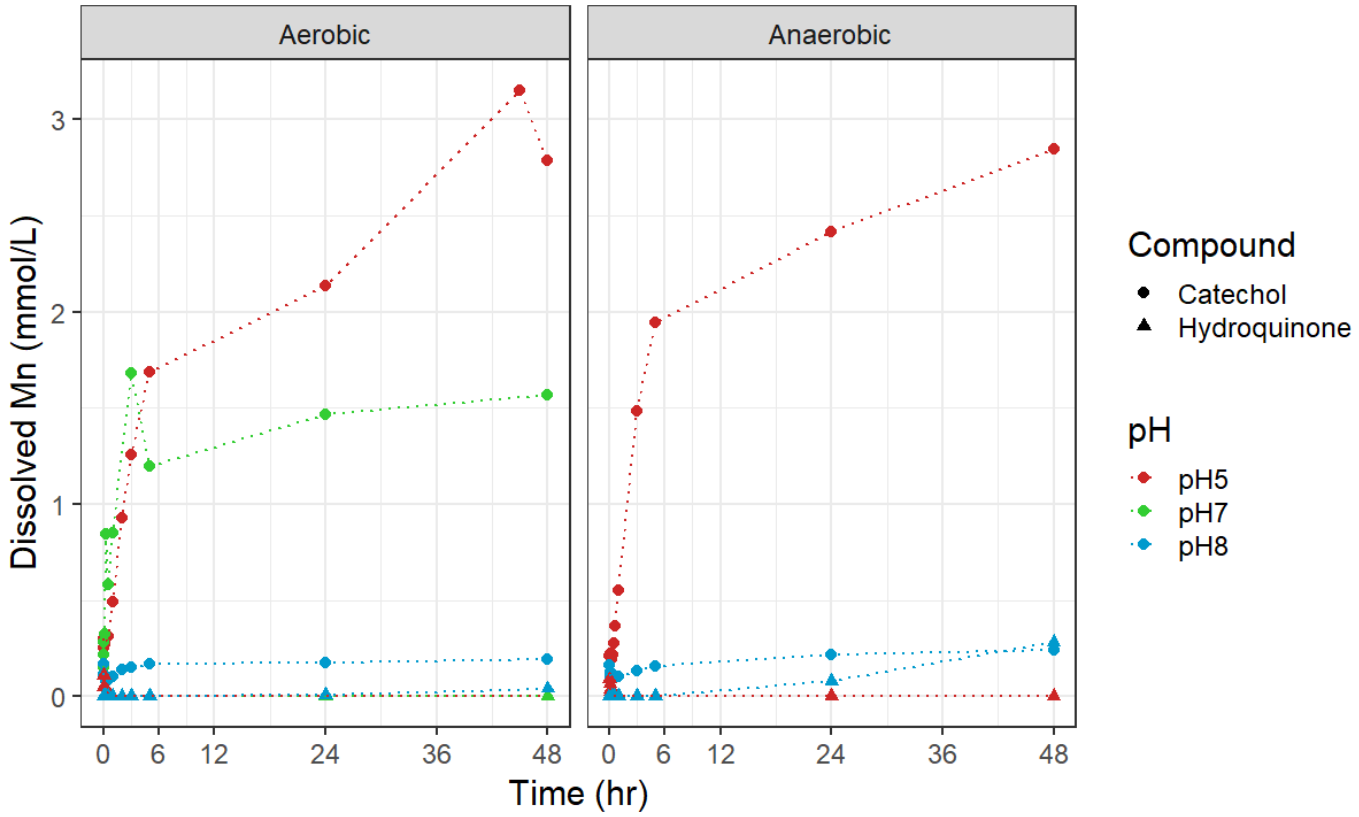

Figure 3.2. Temporal changes in the concentration of dissolved Mn in the supernatant after birnessite reacting with catechol and hydroquinone at different pH condition, under aerobic and anaerobic conditions.

The concentration of dissolved Mn also increases as the reactions progress under both aerobic and anaerobic environments (Figure 3.2). Dissolved Mn should be predominantly Mn^{2+} released after reductive dissolution of birnessite. Though catechols have been found to form

stable Mn^{3+} complexes at alkaline pH (Harrington et al., 2012), these complexes have not been observed to form by dissolution (Akafia et al., 2014). Given that a similar amount of dissolved Mn formed under aerobic and anaerobic conditions, O_2 does not appear to have a large impact on the redox reactions between birnessite and organic compounds. Catechol produces greater dissolved Mn concentrations than hydroquinone at all studied pH conditions, suggesting a more extensive reducing capability of catechol. A significantly larger amount of Mn is dissolved after birnessite reacting with catechol at pH 5 than at pH 7 and 8. This pH dependency agrees well with the increasing trend of the decrease in DOC, suggesting an increasing extent of sorption and redox reactions at lower pH conditions (Stone and Morgan, 1984a). As previously noted, the observed pH effect is related to the ability of the organic molecule to interact with the edge sites of birnessite, which have a positive charge at pH 5 (Balgooyen et al., 2020). Assuming that one mole of catechol will produce one mole of Mn^{2+} (as shown by the reaction mechanism), the formation of 3 mM of Mn^{2+} from the addition of 1mM catechol shows that birnessite further oxidized the products of the initial reaction.

During both catechol and hydroquinone reactions at all experimental pH values, a rapid increase in pH was observed upon commencement of the reaction. The reduction of Mn^{4+} to Mn^{2+} consumes protons, as shown below:

$$MnO_2\ (s) + 4H^+\ (aq) + 2e^- \rightarrow Mn^{2+}\ (aq) + 2H_2O\ (l),$$

The net reaction of Mn-oxide with these organic molecules can be written as:

$$C_6H_6O_2\ (aq) + MnO_2\ (s) \rightarrow Mn^{2+}\ (aq) + C_6H_4O_2\ (aq) + 2OH^-\ (aq)$$

The release of hydroxyls to the reaction solution is expected to occur during the redox reaction. Therefore, both molecules reduced birnessite to some extent, thus generating the observed pH increase. In this study, increases in pH were immediately adjusted to the target pH

values using 1 N HCl. The difference in dissolution efficacy may be related to the ability of catechol to form a bidentate surface complex, thus acting as a chelate that removes Mn atoms from the birnessite crystal structure. However, hydroquinone can only form weak complexes with metal cations and can easily be displaced from the mineral surface by other ions (McBride, 1989a). Additionally, the mechanism proposed by Liu et al., which involved a single electron transfer from hydroquinone to birnessite would result in the formation of Mn^{3+}, and this species would remain in the solid phase. The high average oxidation state and excess of birnessite may have provided enough Mn^{4+} centers to oxidize the hydroquinone present, with negligible amounts of Mn^{3+} reduced to Mn^{2+}. Liu et al. did report formation of Mn^{2+}, but used an initial hydroquinone concentration much higher than the current study (>10 mM) (Liu et al., 2011).

3.3 **Carbon association in solid phase**

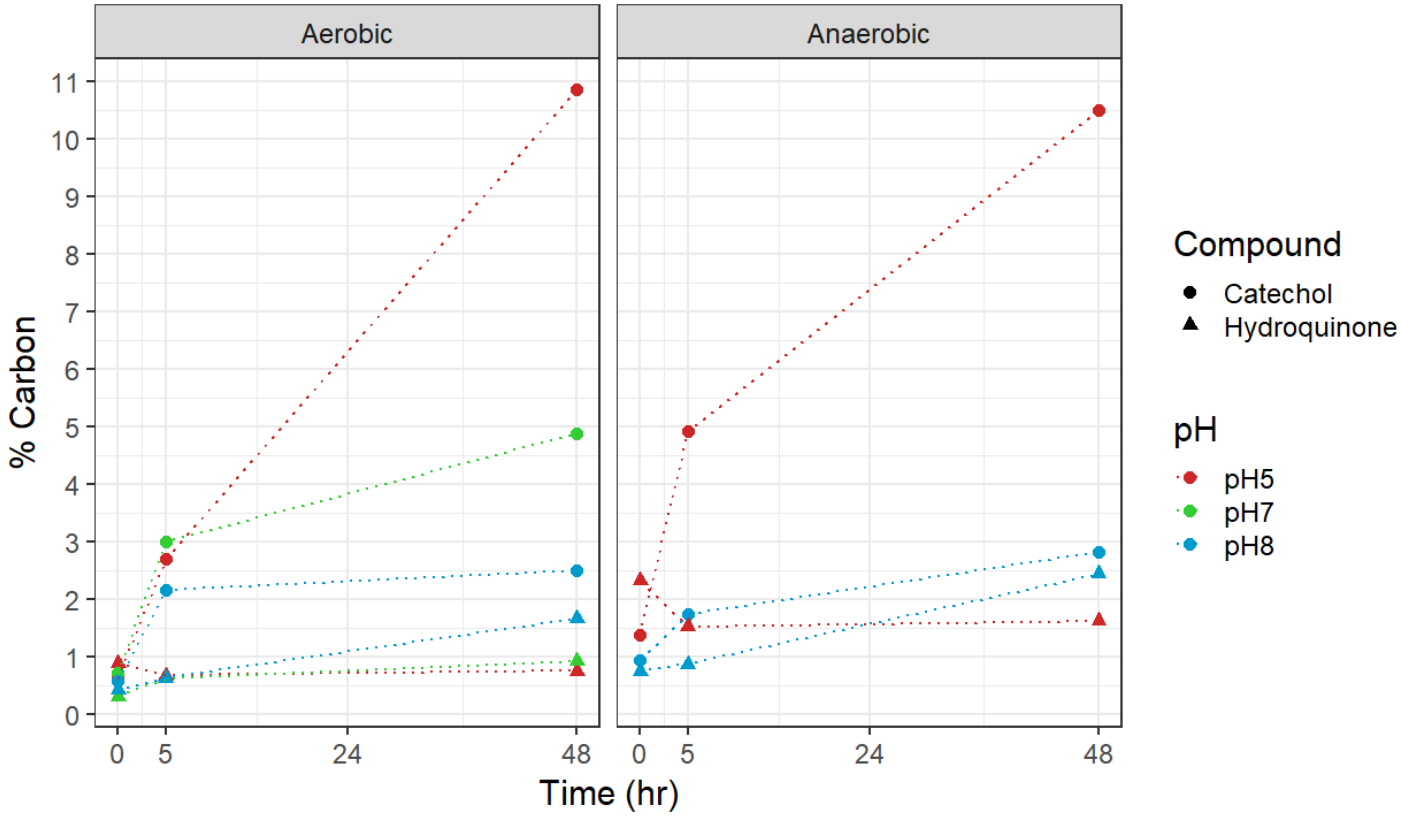

Figure 3.3. Temporal changes in solid phase carbon content (%) during aerobic and anaerobic reactions of catechol and hydroquinone with birnessite at pH 5, 7, and 8

Both molecular structure of the organic compounds and pH influence the amount of carbon associated with the solid phase (Figure 3.3). Similar results were obtained under aerobic and anaerobic conditions. As the reaction progresses, an increasing amount of C was stabilized in the solid phase. In general, more catechol derived C was associated with the birnessite mineral than hydroquinone at all studied pH conditions. Lower pH encouraged C association for both compounds in the preliminary stages of the reaction. For catechol, which formed an appreciable amount of polymeric products at low pH, this pH effect was apparent throughout the duration of the reaction. This aligns with previous findings showing that molecules with higher molecular weight and greater hydrophobicity will be sorbed more than lower molecular weight, hydrophilic species (Allard et al., 2017). Several mechanisms for such an association may exist, including

inner- and outer-sphere complexation, partitioning, and coprecipitation (Di Leo et al., 2012; Gulley-Stahl et al., 2010; Li et al., 2021; McBride, 1989, 1987). These mechanisms may act independently or in tandem to encourage mineral-organic associations.

Catechol is known to form an inner-sphere bidentate surface complex with Mn-oxides (Di Leo et al., 2012), however many studies have previously suggested that these reactions involve the release of the surface-bound organic molecule following the transfer of electron(s) (Johnson et al., 2015; Matocha et al., 2001; Stone, 1987; Stone and Morgan, 1984b). If such a mechanism occurs, it appears that the polymerized reaction products which form during catechol reactions become bound to the birnessite mineral. Product sorption to the birnessite surface did not appear to hinder the progress of the oxidation reaction. This could be caused by a high ratio of birnessite:organic compound, as well as the rapid rate of oxidation relative to the rate of polymer sorption. The observation of a high percentage of carbon in the solid phase appears to coincide with the lack of UV-vis absorbance observed during catechol reactions at pH 5 (discussed below). In both cases, the organic molecules were removed from solution. Still, yield of polymeric products is expected to be greater at pH 8 during catechol reactions based on UV-vis absorbance. Therefore, a similar amount of polymeric products would be expected to associate with birnessite. The reduced negative charge of the birnessite surface at low pH could promote the sorption of reaction products.

Hydroquinone did not appear to form an appreciable amount of coupled products at low pH. At pH 8, when polymerized products did appear in solution, an increase of sorbed C is observed for aerobic and anaerobic conditions. These values are less than but comparable to the amount of C sorbed for catechol at the same pH. These results show the capacity of birnessite to

sorb polymeric molecules which may become stabilized and the promoting effect of low pH during such interactions.

3.4 **Formation of benzoquinones and polymers: Ultraviolet-visible spectroscopy**

The UV-visible spectra of the filtrate samples show clear differences in reaction products that are dependent on time, reaction pH, and molecular structure of the reactants. The promoting effect of birnessite is exemplified by these results, which show rapid oxidation of both catechol and hydroquinone at a rate not observed during control reactions. Past studies have interpreted an increase in absorbance across a range of wavelengths extending towards 800 nm to be indicative of the formation of humic-like polymers (Hardie, 2008; Larson and Hufnal Jr., 1980; Shindo and Huang, 1992; Wang and Huang, 1989). Particularly, absorbance at 400 and 600 nm has been shown to be directly related to the yield of humic polymers(Shindo and Huang, 1984). The formation of such substances can be seen visually as the development of a brown color in the solution, giving rise to this increased light absorption. Solutions of pure catechol and hydroquinone do not absorb visible light, as observed here and by others (Colarieti et al., 2006).

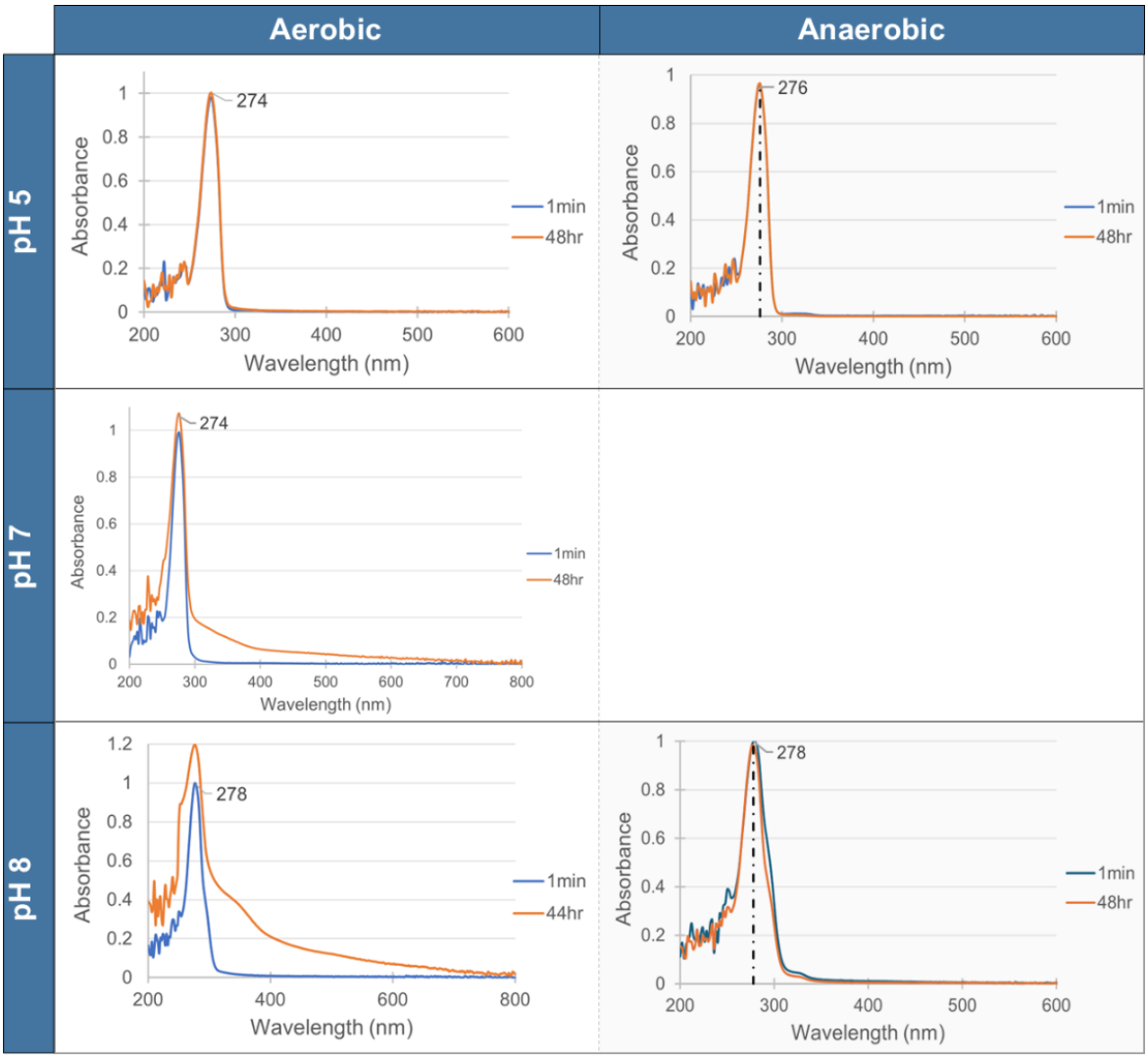

Figure 3.4.1: UV-vis spectra for catechol control reactions at varying pH under aerobic and anaerobic conditions.

The spectra obtained during control reactions of 1mM catechol in the absence of birnessite are shown in Figure 3.4.1. These reactions were conducted to examine the autoxidation of catechol over time and at varying pH conditions. Reference catechol solutions prepared at a concentration of 1mM exhibit a single peak with a λ_{max} at about 275 nm. Here, we find that at pH 5, no oxidation of the catechol solution occurs after exposure to air for a period of 48 hours. As the pH is increased from 5 to 7, a higher absorbance is recorded at 275 nm accompanied by an increased absorbance at higher wavelengths. Increasing the pH to 8 further encourages this

increased absorbance, and a shoulder begins to appear near 256 nm (to be discussed later). This suggests that under aerobic conditions, high pH values encourage the autoxidation and coupling of catechol molecules. Molecular oxygen and hydroxyl species could both be involved in oxidizing catechol in the absence of birnessite (Chang Chien et al., 2009; Larson and Hufnal Jr., 1980; McBride, 1987; Pillar-Little et al., 2014). However, under anaerobic conditions we find that even at high pH, there is much less formation of coupled products as indicated by the absence of absorbance in the range of 400-600 nm.

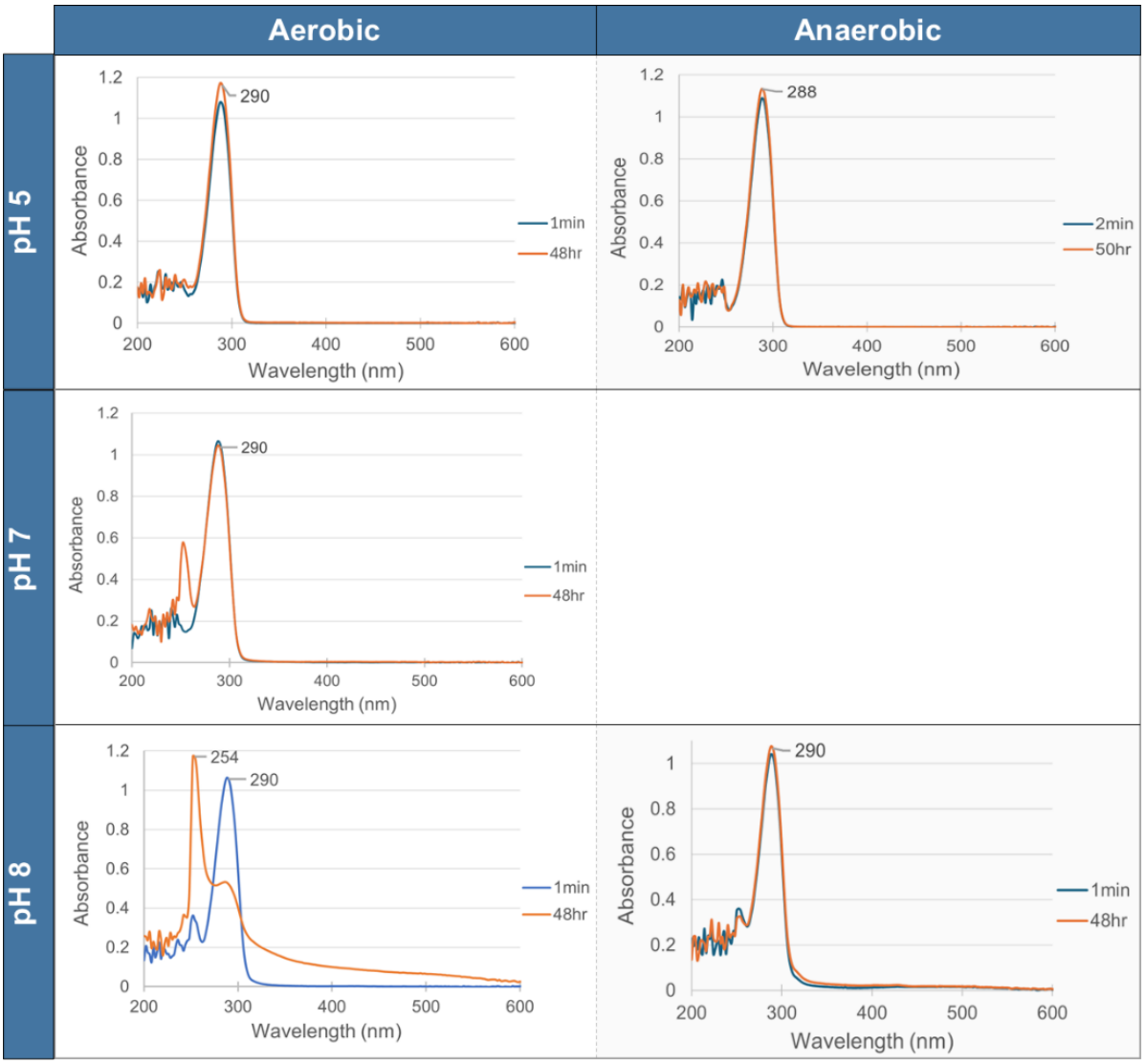

Figure 3.4.2: UV-Vis spectra for hydroquinone control reactions at varying pH under aerobic and anaerobic conditions.

Similar to catechol control, reference hydroquinone solutions prepared at a concentration of 1mM exhibit a single peak with a λ_{max} at about 290 nm (Figure 3.4.2). An increase in absorbance from 1.05 to 1.18 at this wavelength at pH 5 may indicate coupling or oxidation to a small degree in both aerobic and anaerobic atmospheres. Higher pH values show conversion of hydroquinone into p-benzoquinone over time in the presence of oxygen. Test solutions of 1 mM p-benzoquinone confirmed the identity of this new peak with λ_{max} = 254 nm (spectra not shown). Similar to catechol under aerobic conditions, we find an increased absorbance at higher

wavelengths which suggests oxidative coupling. Hydroquinone appears largely unaltered at pH 8 under anaerobic conditions, showing that atmospheric oxygen is involved in the autoxidation of hydroquinone.

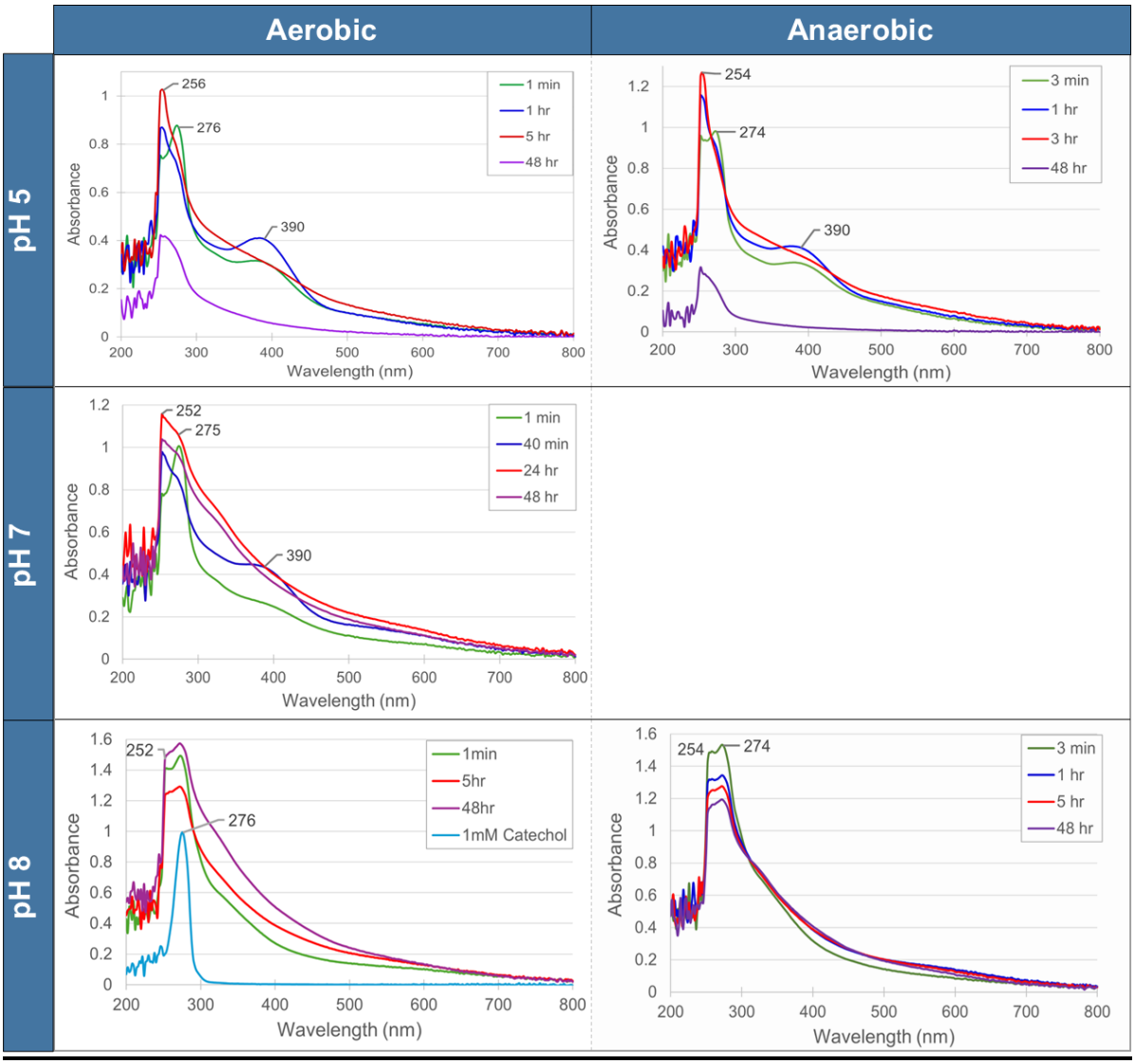

Figure 3.4.3: UV-vis spectra for the supernatant in birnessite-catechol reactions at varying pH under aerobic and anaerobic conditions. A 1mM catechol reference spectrum has been included in the aerobic pH 8 spectra for reference.

As shown in Figure 3.4.3, birnessite rapidly converts catechol into oxidized products and encourages the formation of polymerized products. The broad peak visible in the pH 5 and pH 7 spectra at 390 nm has previously been attributed to the formation of o-benzoquinone (Matocha et

al., 2001). Absorbance at this wavelength gradually increases within the first hour of the reaction, indicating that this is the initial product formed during the redox reaction. Approaching five hours, the o-benzoquinone peak wanes and gives rise to increased absorbance at other wavelengths, particularly extending towards 250 nm. The conversion of benzoquinone into new products is indicated by the presence of two isobestic points above and below the peak at 390 nm. The loss of o-benzoquinone is likely related to coupling reactions which cause the observed increase in absorbance at many wavelengths extending towards 250 and 600 nm. The absence of this peak during pH 8 reactions shows that the o-benzoquinone product either does not form, or reacts rapidly to form coupled products. The higher absorbance at 400 and 600 nm even after one minute of reaction suggests that the coupling of reaction products is rapid. Over time, these coupled products continue to accumulate at high pH. Interestingly, at pH 5 the reaction solution became clarified after 24 hours, reflected by a decrease in absorbance across all wavelengths for the 48 hour sample. This change indicates that the brown humic-like polymers formed during the first 5 hours were somehow lost from solution. There are several possibilities that could explain the loss of products, however none of them can be determined conclusively through UV-vis alone. For one, there could have been further degradation and conversion to aliphatic forms or CO_2. A second possibility is the sorption of these molecules to the birnessite mineral. In this case, products associated with the solid phase would have been removed during filtration.

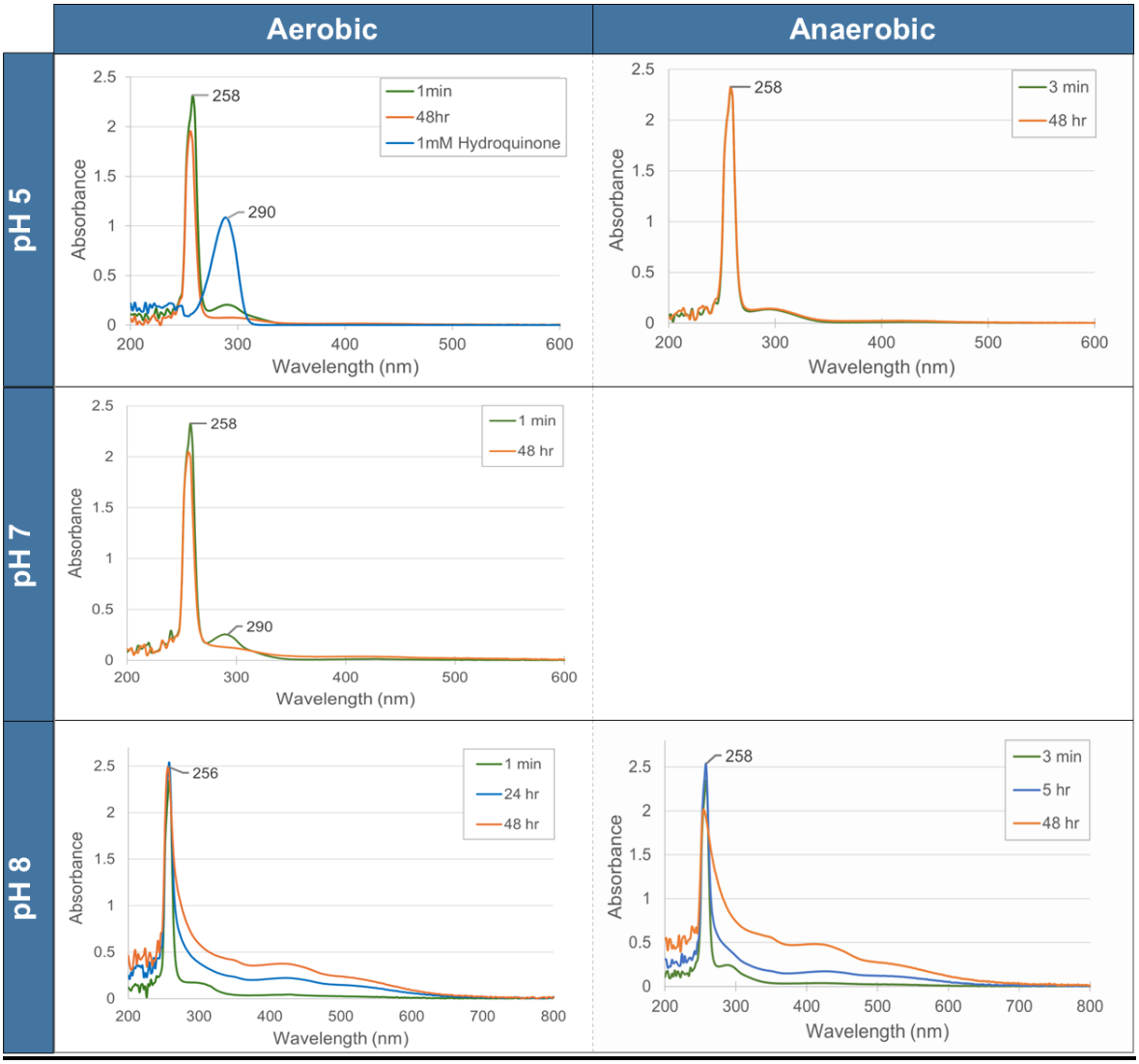

Figure 3.4.4: UV-vis spectra for the supernatant in birnessite-hydroquinone reactions at varying pH under aerobic and anaerobic conditions. A 1mM hydroquinone reference spectrum has been included in the aerobic pH 5 spectra for comparison.

The UV-vis results for the birnessite-hydroquinone reactions are summarized by the spectra in Figure 3.4.4. In each case, rapid conversion to p-benzoquinone has been observed and this was not dependent on the presence of oxygen. The fact that p-benzoquinone in solution interacts more strongly with light compared to catechol or hydroquinone is shown by the higher absorbance. A test solution of 1 mM p-benzoquinone provided a maximum absorbance at 258 nm. This aligns with the findings of Stone and Morgan (Stone and Morgan, 1984a), who

previously stated that p-benzoquinone is the most likely oxidation product of the reaction between hydroquinone and Mn-oxide. However, it should be noted that for both catechol and hydroquinone reactions, the benzoquinone product is not the only possible immediate oxidation product. In fact, it is suspected that these reactions also form semiquinone species, aliphatic fragments, and CO_2 (Majcher et al., 2000; Naidja et al., 1998). At pH 5 and pH 7, the spectra remained largely unchanged throughout the reaction period, despite the fact that quinone and semiquinone compounds are expected to be highly reactive and readily participate in coupling and polymerization (Naidja et al., 1998; Stevenson, 1982; Swan, 1974). It appears that a high pH is important for encouraging the formation of polymeric products during birnessite-hydroquinone reactions. The increase in absorbance at pH 8 over the entire reaction period indicates that the coupled products formed remained in solution. As previously observed, higher pH limits the affinity of polymerized species for the surface of birnessite.

3.5 **Characterization of mineral-OC associations using ATR-FTIR**

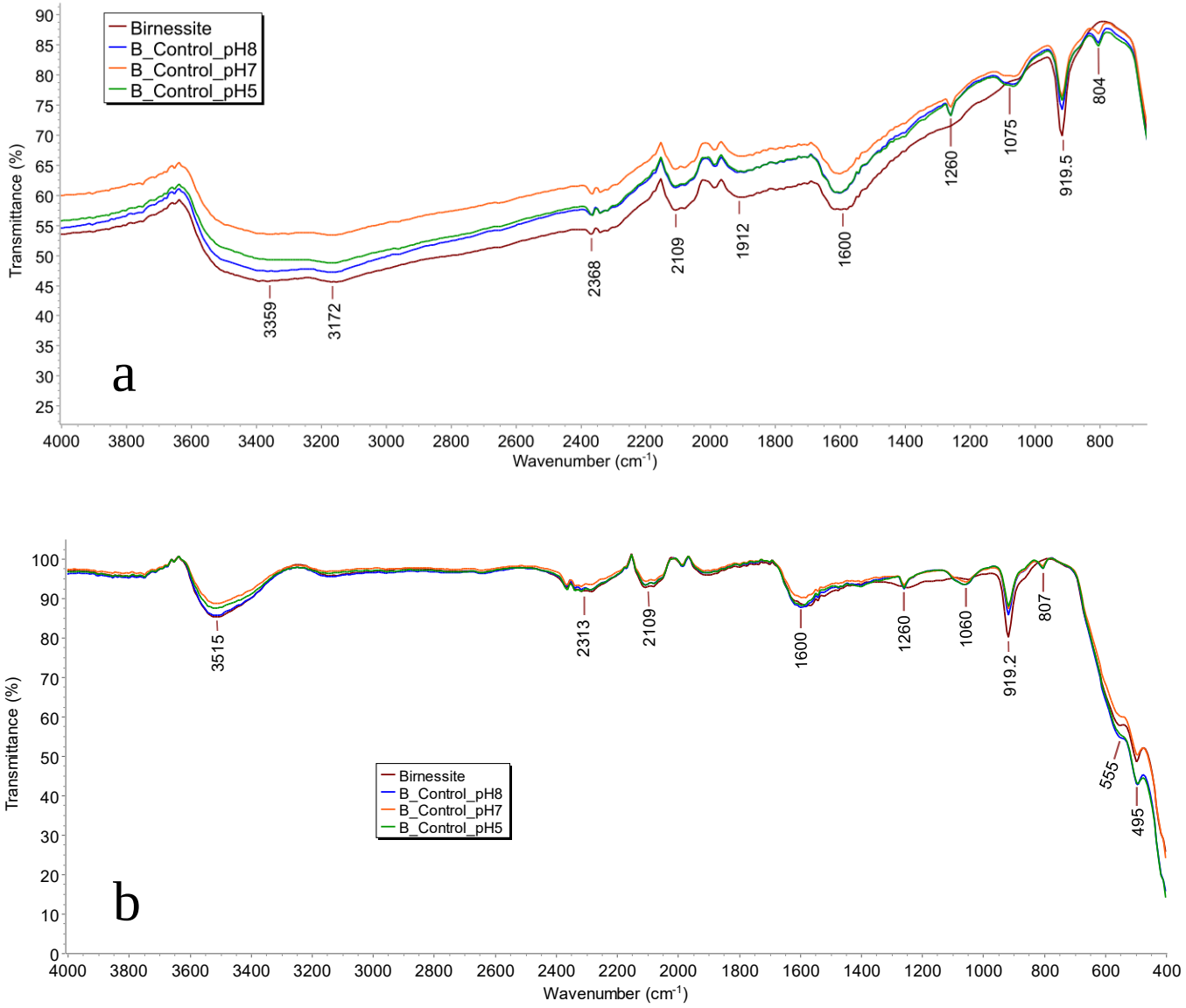

Figure 3.5.1: (a) FTIR spctra of unreacted birnessite and of birnessite controls at pH 5, 7, and 8. (b) Identical spectra after baseline correction.

The FTIR spectrum of unreacted birnessite can be found in Figure 3.5.1. The broad absorption band at 3515 cm^{-1} is attributed to the stretch vibration of -OH within the crystallographic structure of birnessite (Potter and Rossman, 1979), while the band at 1630 cm^{-1} is caused by the -OH bend vibrations of adsorbed water molecules (Hardie, 2008; Liu et al., 2011; McBride, 1989). The peaks at 2313 cm^{-1} and 2109 cm^{-1} are not characteristic of birnessite

but are likely caused by background interference given that they also appear in the organic spectra (shown below), albeit to a lesser extent. The strong absorption band which appears at 919 cm^{-1} does not appear to be consistently detected by previous researchers. Mcbride (1989) discusses the presence of this peak, but concludes that it is not characteristic of birnessite and may instead be a feature of the hydrated surface since it diminishes upon heating the oxide to 100℃ (McBride, 1989). Zhao et al. (2012) indicate that this feature is caused by the bending vibration of -OH located at vacancies (Zhao et al., 2012). The shoulder present at 555 cm^{-1} and the peak at 495 cm^{-1} are due to the Mn-O lattice vibrations of birnessite (Hardie, 2008; McBride, 1989). The spectra for birnessite controls were nearly identical at each pH condition, however they differed from the original birnessite sample in three locations: two small peaks at 807 and 1260 cm^{-1} and a small, broad peak centered at roughly 1075 cm^{-1}. Given that the birnessite in these control samples was not reacted with any organic molecule, these features are likely associated with sorption of water molecules given that freeze-drying alone will not remove all water. However, it should be noted that absorbance near 1075 cm^{-1} has been attributed to the formation of $MnCO_3$, though this is expected to be accompanied by peaks at 860 and 725 cm^{-1} (Hardie, 2008).

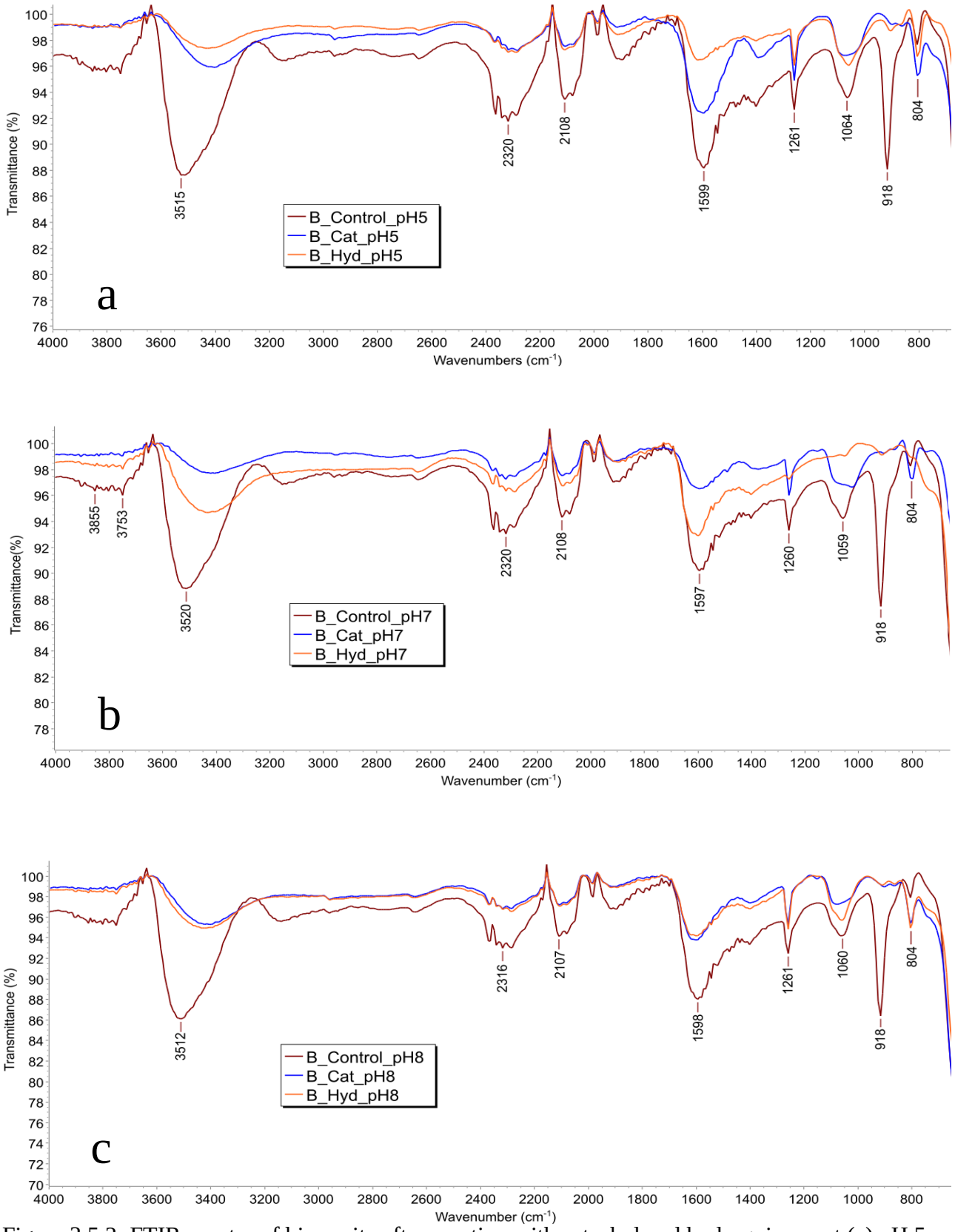

Figure 3.5.2: FTIR spectra of birnessite after reaction with catechol and hydroquinone at (a) pH 5, (b) pH 7, and (c) pH 8. Spectra obtained for control reactions at each pH are included for reference.

The spectra presented in Figure 3.5.2 allow for comparison of the birnessite samples after reaction with catechol and hydroquinone at a given pH. Since variation in spectra across time points was minimal, the spectra obtained for samples of the same experiment have been averaged. Differences in peak intensity are not expected to indicate significant differences between the reactions. Overall, it was observed that the FTIR spectra of the birnessite samples reacted with catechol and hydroquinone were similar to each other and to the control at each pH, except for the absence of a peak at 917 cm^{-1} for birnessite samples that have been reacted with diphenols. Reasoning that MnO_6 edge-sharing octahedra are similar to AlO_6 edge-sharing octahedra of clay minerals, Zhao et al. explains that an absorption band between 911 – 917 cm^{-1} should be observed in both cases for -OH bend vibrations at vacancies within the crystal structure. Upon sorption of Pb^{2+} to birnessite, this band shifts to lower wavenumbers (Zhao et al., 2012). However, the absence of this band in our spectra may indicate that these -OH groups were subject to ligand exchange upon formation of a surface complex by the catechol and hydroquinone molecules.

3.6 **Transformation of catechol and hydroquinone: FTIR**

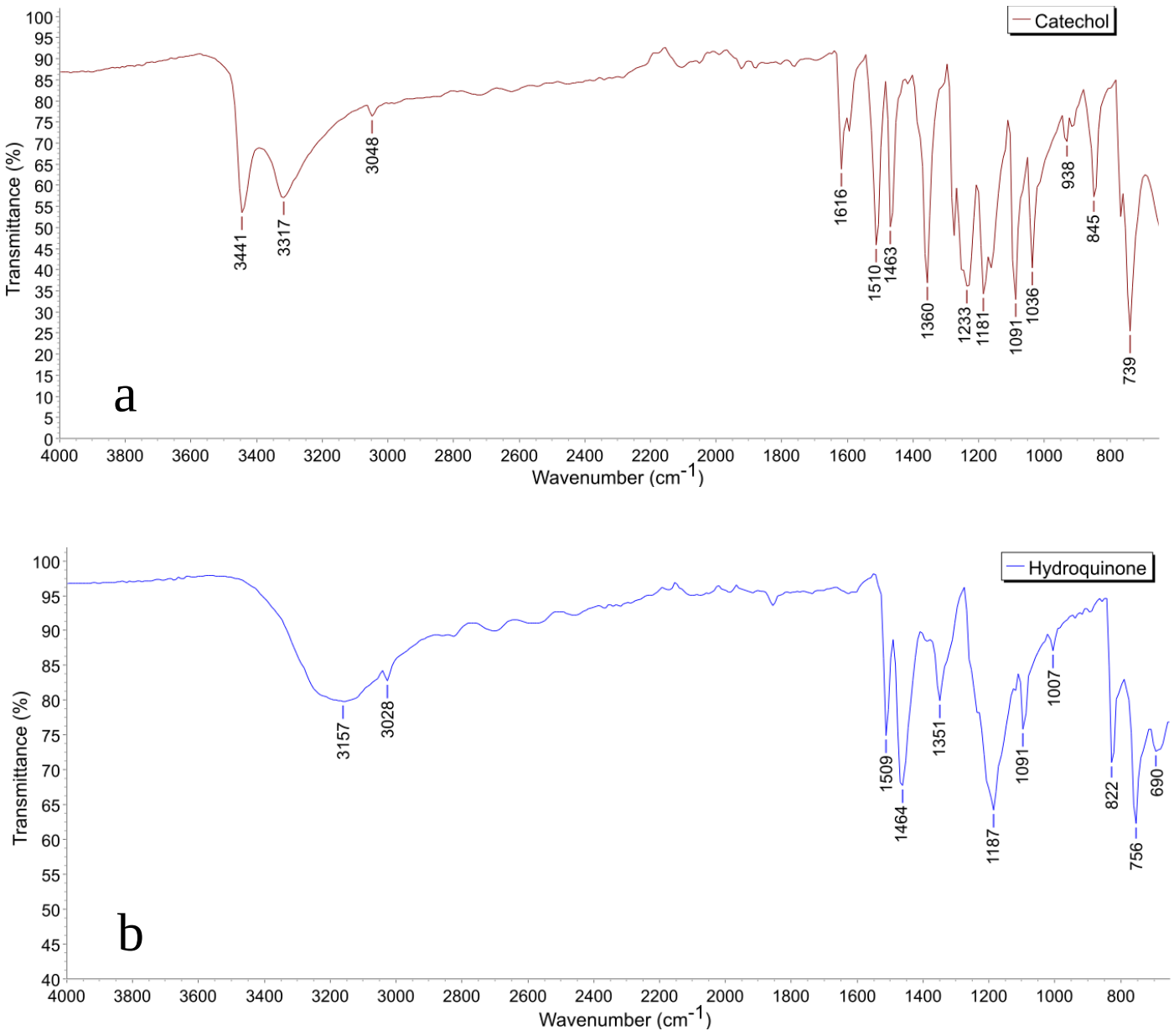

Figure 3.6.1: FTIR spectra of (a) catechol and (b) hydroquinone.

Table 3.6.1: Peak assignments for pure catechol and hydroquinone

Compound	Wavenumber (cm^{-1})	Assignment
Catechol	3441, 3317	ν(O-H)
	3048	ν(C-H)
	1616, 1510 1463, 1360	ν(C=C)
	1233	δ(C-H)
	1181	δ(O-H)
	1095, 1036	δ(C-H)
	918, 849	ρ(C-H)
	769	ν(C=C)
	741	ρ(C-H)
Hydroquinone	3157	ν(O-H)
	3028	ν(C-H)
	1509, 1464, 1351	ν(C=C)
	1187	δ(O-H)
	1091	δ(C-H)
	822	ρ(C-H)
	756	ν(C-O), ρ(O-H)
	690	ρ(C-H)

ν – stretching, δ – in plane bending, ρ – out of plane bending
(Aktas et al., 2003; Kubinyi and Keresztury, 1997; Pillar-Little et al., 2015; Ramírez and López Navarrete, 1993; Selvaraj et al., 2019)

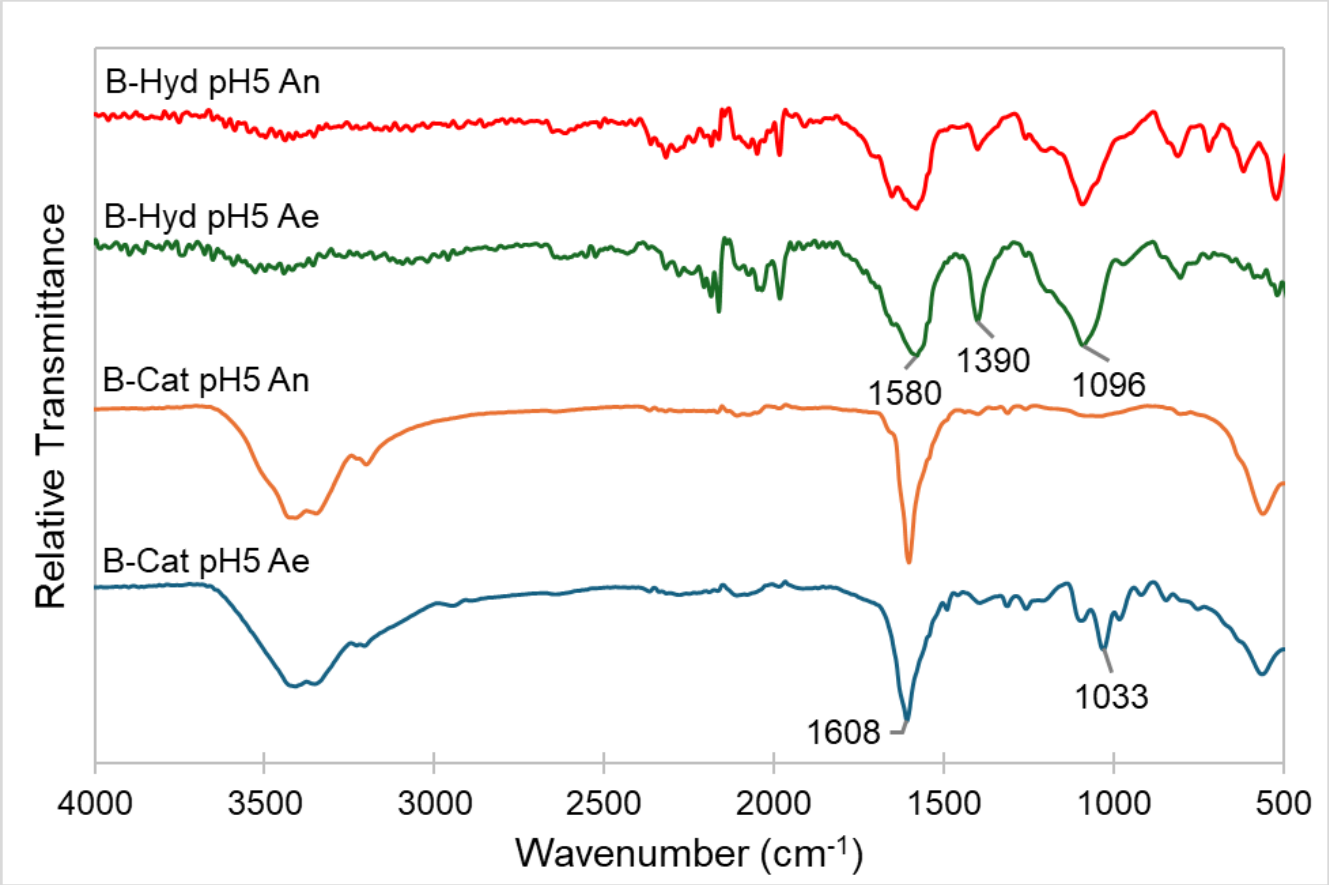

Figure 3.6.2: FTIR spectra of supernatants from birnessite-catechol (B-Cat) and birnessite-hydroquinone (B-Hyd) reactions at pH 5 under aerobic (Ae) and anerobic (An) conditions

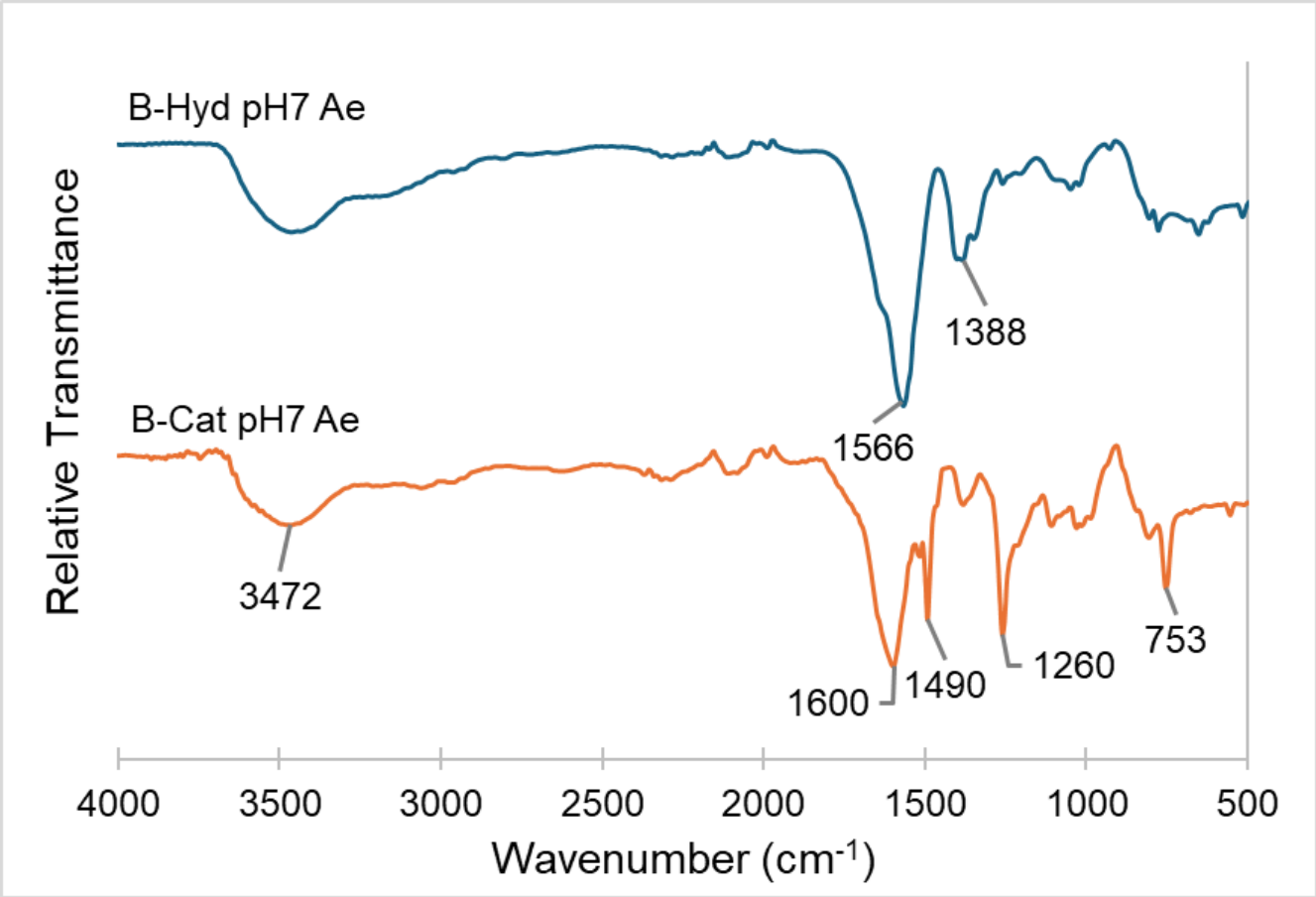

Figure 3.6.3: FTIR spectra of supernatants from birnessite-catechol (B-Cat) and birnessite-hydroquinone (B-Hyd) reactions at pH 7 under aerobic (Ae) conditions.

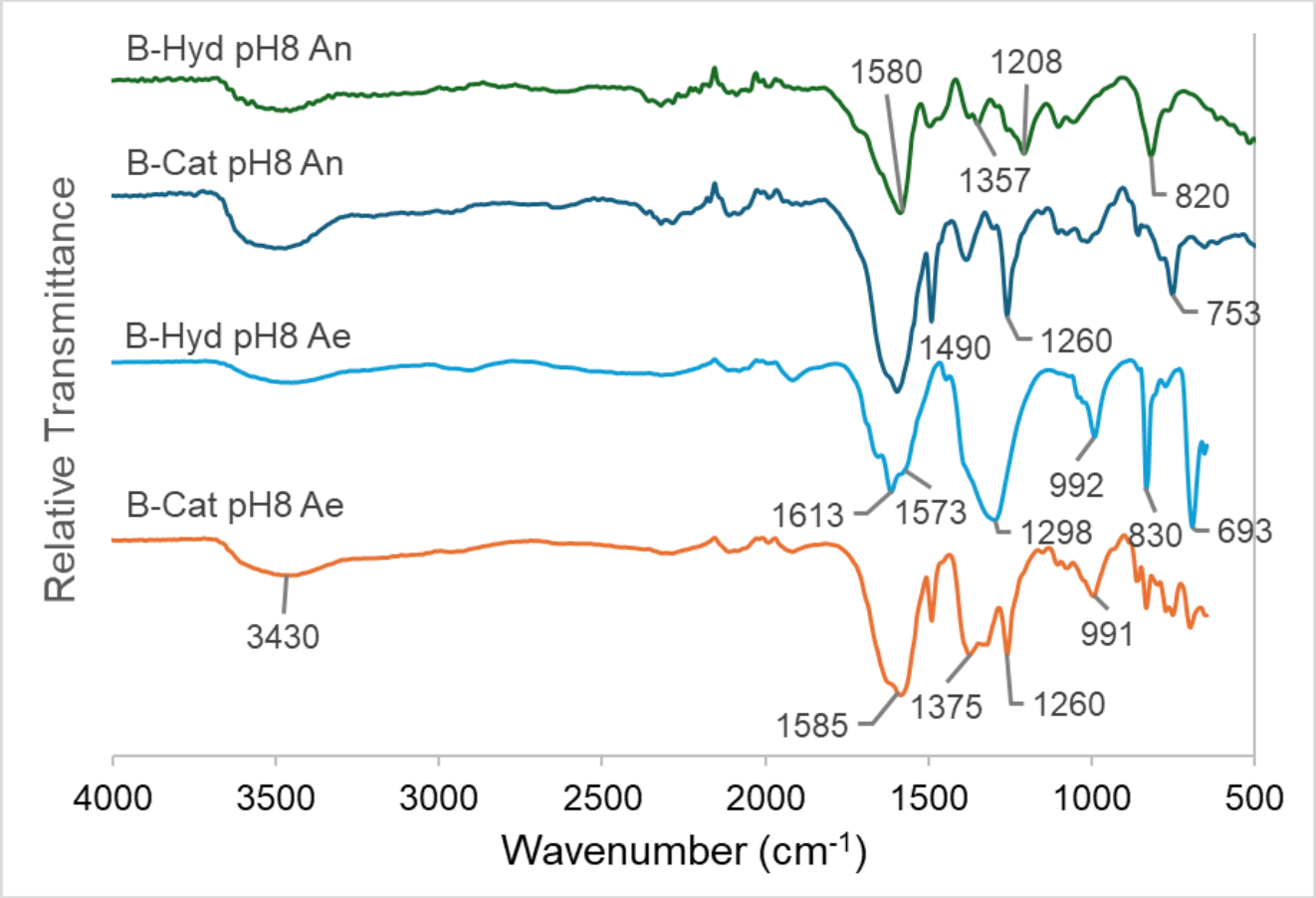

Figure 3.6.4: FTIR spectra of supernatants from birnessite-catechol (B-Cat) and birnessite-hydroquinone (B-Hyd) reactions at pH 8 under aerobic (Ae) and anerobic (An) conditions.

Table 3.6.2: Peak assignments for birnessite-catechol supernatants

Experiment	Wavenumber (cm^{-1})			Assignment
	pH 5	pH 7	pH8	
B-Cat	3411 3355	3472	3444	ν(O-H)
	3206			ν(O-H)
		3060 (w)		
	2947 (w)	2967 (w)		aliphatic δ(C-H)
	1608	1600	1620 (sh)	aromatic ν(C=C)
			1585	ν(C=C) symmetric δ(C-O in COO^-)
	1492	1491	1491	ν(C=C), δ(C-O-H)
	1397	1382	1375	δ(O-H), ν(C=C), asymmetric δ(C-O in COO^-)
	1316		1325	δ(C=C-H)
	1260	1256	1260	ν(C-O), δ(C-H)
		1108	1102 (w)	δ(O-H)
	1097		1075 (w)	δ(C-H)
	1033	1030		δ(C-H)
	978		996	
	921			
	846 (w)	804	831	
	753	750	752	

ν – stretching, δ – in plane bending, ρ – out of plane bending,
B-Cat = Birnessite-Catechol
sh = shoulder, w = weak
(Gulley-Stahl et al., 2010; Hardie, 2008; Pillar-Little et al., 2015)

Table 3.6.3: Peak assignments for birnessite-hydroquinone supernatants

Experiment	Wavenumber (cm^{-1})			Assignment
	pH 5	pH 7	pH8	
B-Hyd	3209	3465	3335	ν(O-H)
		2964 (w)	2971	aliphatic ν(C-H)
			2903	aliphatic ν(C-H)
		1620 (sh)	1612	aromatic ν(C=C)
	1580	1566	1580	ν(C=C), δ(C-O in COO^-)
	1402			ν(C=C)
		1386		asymmetric δ(C-O in COO^-)
			1311	δ(C=C-H)
	1260 (w)	1256		ν(C-O), δ(C-H)
	1196 (sh)			
	1092	1094 (sh)		
		1049		δ(C-H)
		1020		δ(C-H)
	975		992	
	804		830	
		774	775	
			695	
		652		

ν – stretching, δ – in plane bending, ρ – out of plane bending,
B-Hyd = Birnessite-Hydroquinone
sh = shoulder, w = weak
(Kubinyi and Keresztury, 1997; Liu et al., 2011; McBride, 1989)

The FTIR spectra of the freeze-dried supernatants are most consistent with a combination of aromatic, carboxylic, and aliphatic functional groups. Only small variation existed across time points within the same experiment. As such, the spectra for samples within the same experiment were averaged and baseline corrected to produce these plots. The absence of variation over time has been previously reported in a study of catechol polymerization using surface-enhanced Raman spectroscopy (Sánchez-Cortés et al., 2001).

The peaks observed in Figures 3.6.1-4 are summarized in Tables 3.6.1-3. The absorption bands observed from 3500 – 3200 cm^{-1} are attributed to stretching vibrations of hydroxyl groups, and are a common feature of alcohols, phenols, and carboxylic acids. Stretching vibrations of methyl and methylene groups were found near 2900 cm^{-1} for both catechol and hydroquinone reactions, and identification of these groups is corroborated by NMR results (Section 3.7). Multiple samples have an absorption band just above 1600 cm^{-1}, which is caused by the presence of C=C bonds of aromatic rings. Likewise, this assignment may also be made for absorption bands near 1580 cm^{-1}. However, multiple authors (Hardie, 2008; Liu et al., 2011; McBride, 1987) note that the band at 1580 cm^{-1} is due to the symmetric stretch of the C-O bond in carboxylate anions. In many of the observed spectra, the peak in this region is broad and may be composed of contributions of both of these functional groups. An example of this can be seen in the spectra of the pH 8 aerobic reactions (Figure 3.6.4). In catechol spectra, the band at 1490 cm^{-1} is also attributed to the C=C bond of the aromatic ring. Naidja et al. state that absorption bands near 1486 cm^{-1} are characteristic of ortho-substituted aromatics (Naidja et al., 1998).

The combination of bands at around 1580 and 1380 cm^{-1} are often considered to be evidence of carboxylate groups formed during the oxidation of the phenols (Liu et al., 2011; Naidja et al., 1998). Appearance of peaks near 1710 cm^{-1}, which are characteristic of carboxylic acids, may be

related to whether an acidic extraction procedure is performed to isolate the humic acids formed. In a report by Liu et al., these features did not show up until acidification of the supernatants (Liu et al., 2011). Since no such extraction procedure was performed in our case, this may explain the absence of a band near 1710 cm^{-1} despite the formation of carboxyl functional groups. Lastly, absorption near 1260 cm^{-1} is likely related to the stretching vibration of C-O bonds. Aliphatic carboxylic acids including maleic, oxalic, and cis,cis-muconic acids have similar absorption bands in their respective FTIR spectra (Pillar-Little et al., 2015). However, a C-O bond may also be evidence of the formation of ether linkages between oxidized products (Hardie, 2008), especially considering that the C-O stretch of pure catechol/hydroquinone does not absorb at this wavenumber. The spectra for catechol at pH 5, a reaction condition which provided evidence of polymerization in other analyses, was generally devoid of signals related to carboxylic functional groups (Figure 3.6.2). This signal could be dominated by the aromatic stretch of polymeric species. The additional peak near 1030 cm^{-1} in the presence of oxygen could indicate presence or absence of ether linkages based on oxygen availability. This difference has been postulated to arise from the presence/absence of radical species (Swan, 1974).

No obvious trend was observed for the formation of differing functional groups depending on the reaction conditions of pH, oxygen availability, and starting compound. It should be noted that for catechol at pH 5, which showed evidence of polymerization in other analyses, there is a general lack of absorption bands that would be associated with aliphatic/carboxylic functional groups. Our FTIR results appear to support the notion that birnessite is able to oxidize catechol and hydroquinone to an array of degradation products including aliphatic fragments and polymeric species.

3.7 **Identification of major degradation products: NMR**

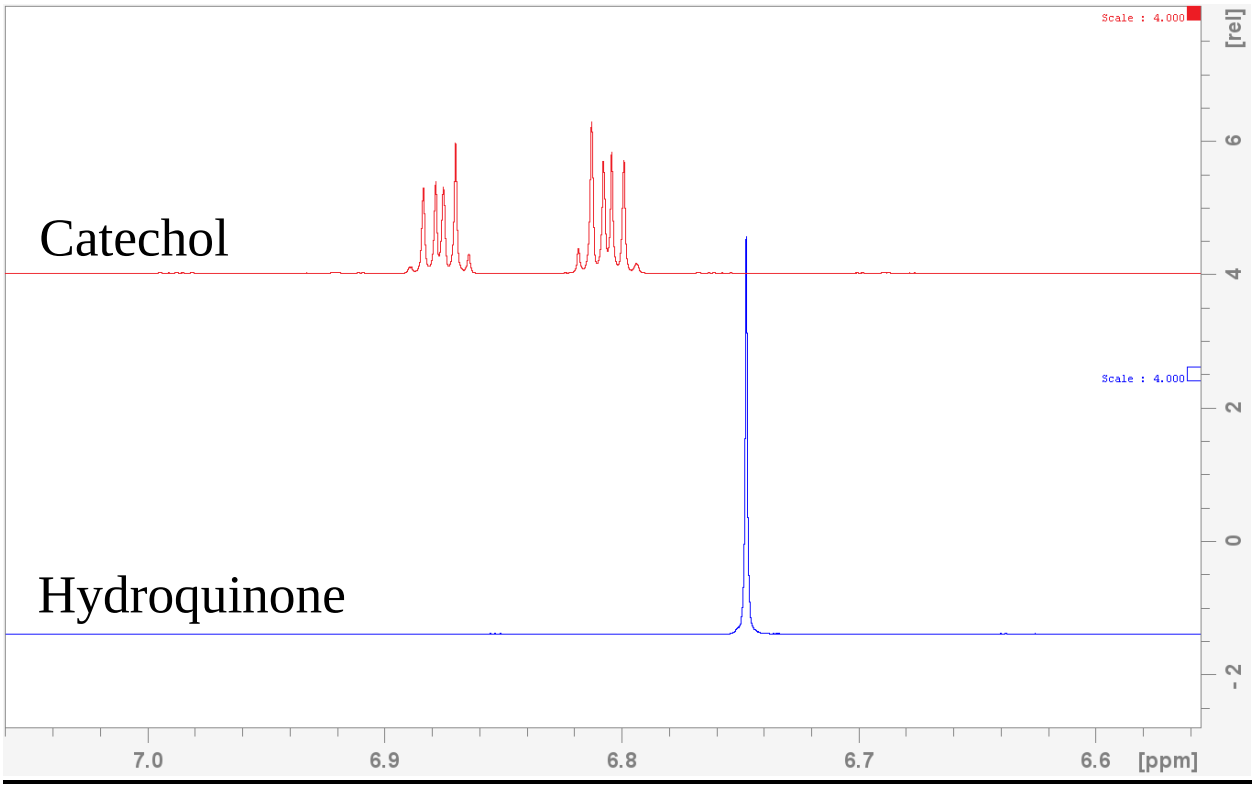

Figure 3.7.1. Reference NMR spectra for 1mM catechol (red) and hydroquinone (blue).

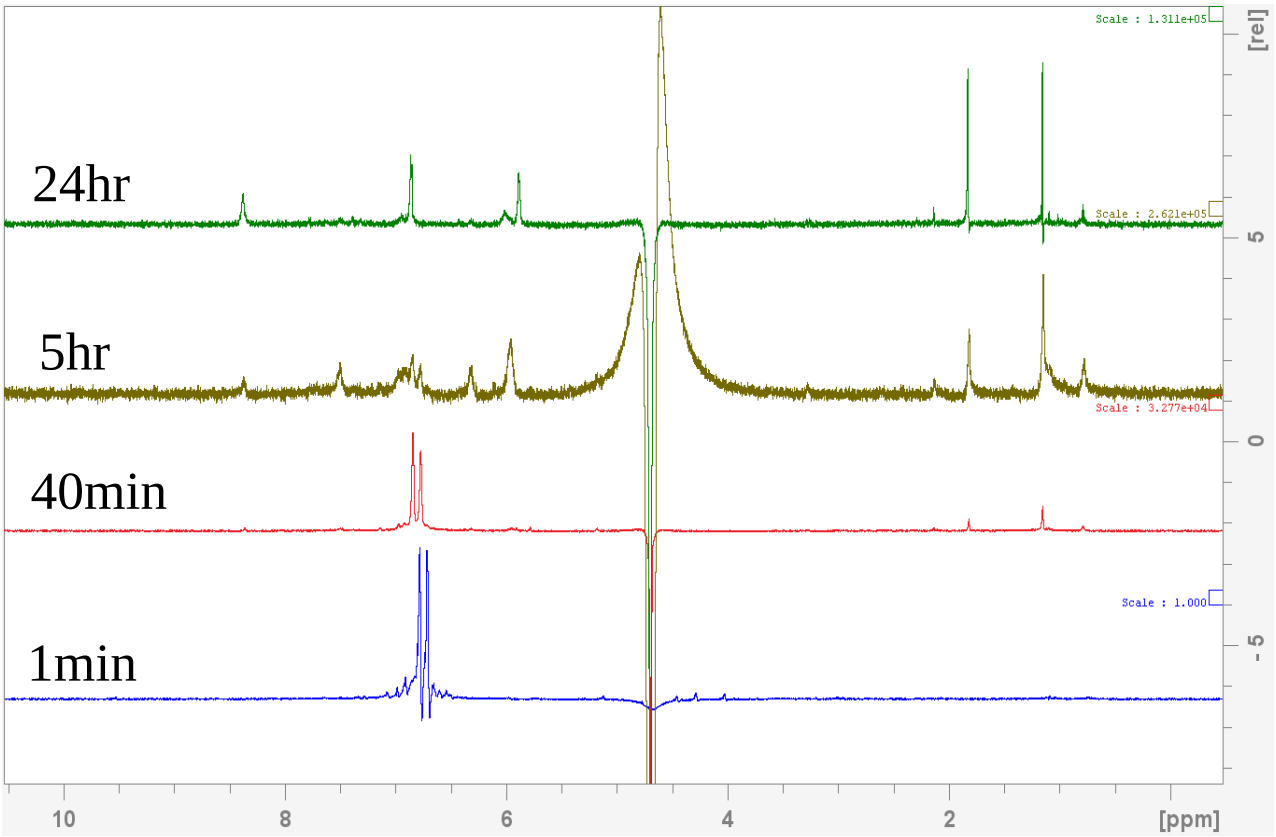

Figure 3.7.2. ^{1}H NMR spectra of supernatant from birnessite-catechol reaction at pH 5 under aerobic conditions. Large peaks at 4.70 ppm are from ^{1}H in H_2O.

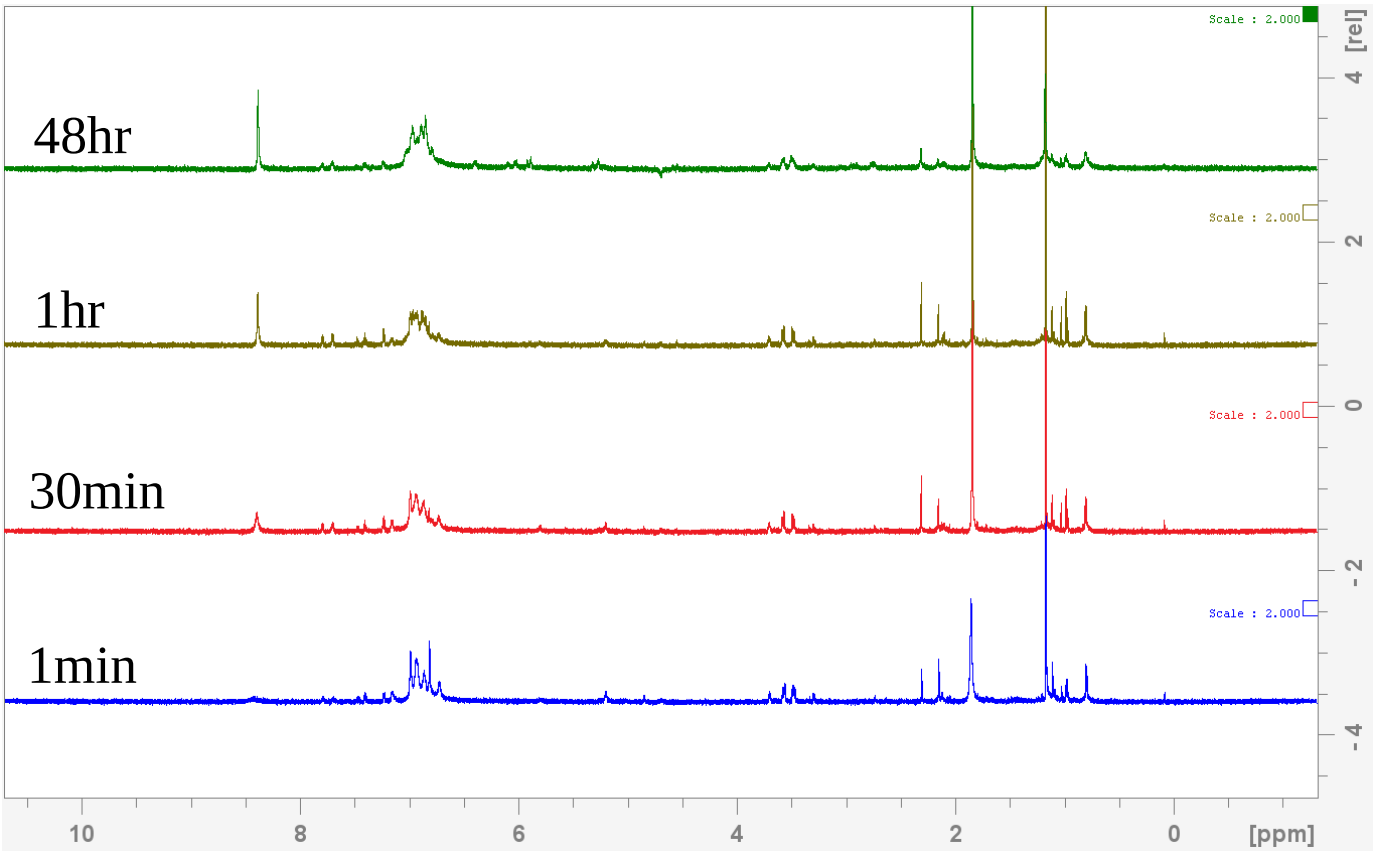

Figure 3.7.3. ^{1}H NMR spectra of supernatant from birnessite-catechol reaction at pH 8 under aerobic conditions.

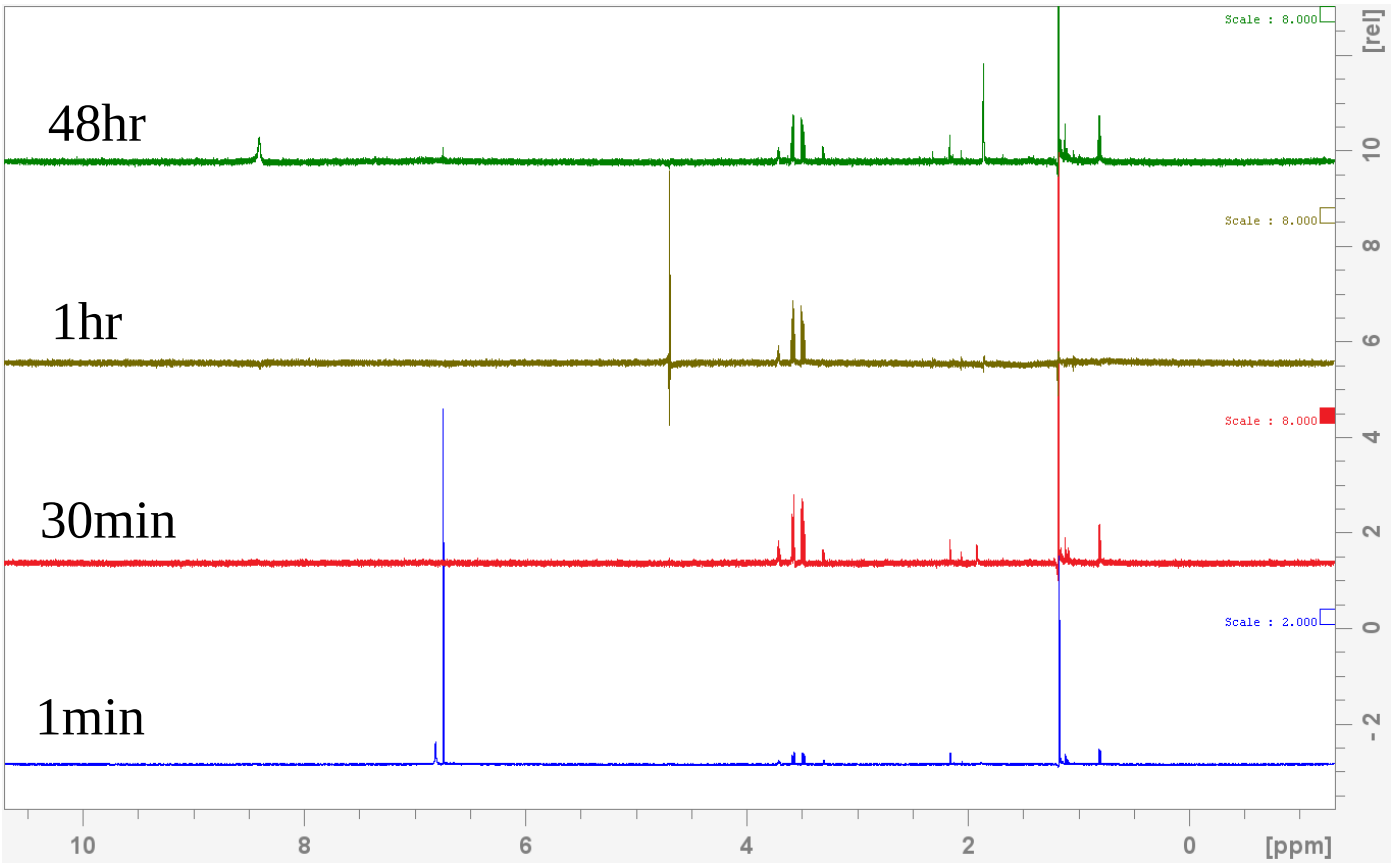

Figure 3.7.4. ^{1}H NMR spectra of supernatant from birnessite-hydroquinone reaction at pH 5 under aerobic conditions. Large peaks at 4.70 ppm are from ^{1}H in H_2O.

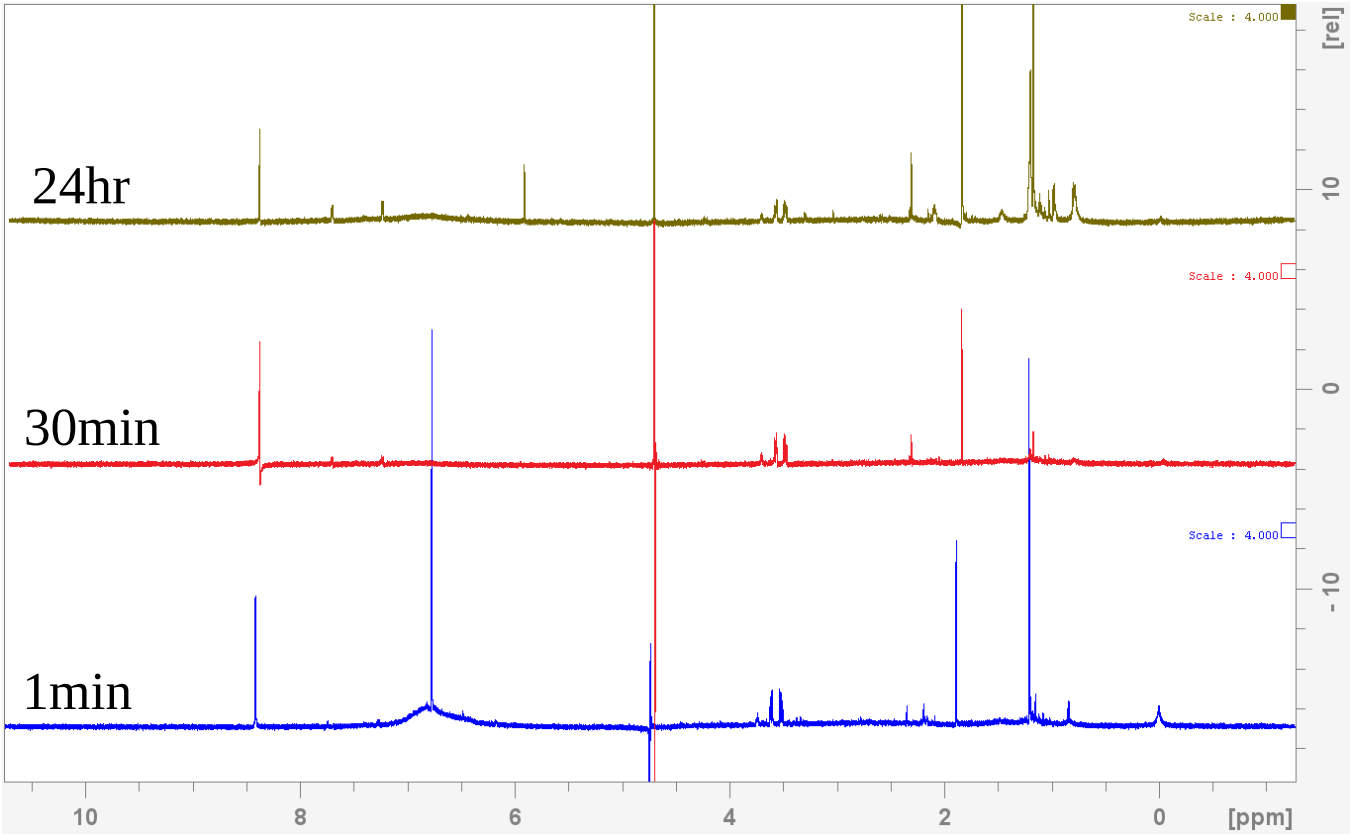

Figure 3.7.5. ^{1}H NMR spectra of supernatant from birnessite-hydroquinone reaction at pH 8 under aerobic conditions.

Solution state ^{1}H NMR was employed to glean further information on the specific oxidative degradation products formed during the reactions at acidic and alkaline conditions. Though many studies have turned to NMR in efforts to characterize the structure of natural organic matter in soils, these have mostly been CPMAS ^{13}C NMR to provide general knowledge of the type of compounds present and quantify the relative amounts of aromatic:aliphatic constituents (Gerke, 2018). However, some have successfully utilized NMR techniques to propose tentative formulae for humic acids (Simpson et al., 2001). Still, very few studies have attempted to identify degradation products of phenolic compounds upon reaction with manganese oxides and this remains a knowledge gap in these studies.

The characteristic NMR spectra for pure catechol and hydroquinone can be found in Figure 3.7.1. The catechol spectrum is comprised of two sets of multiplets centered at 6.8 and 6.88 ppm, while hydroquinone has a singlet at 6.74 ppm. We observe that during birnessite-catechol reactions (Figures 3.7.2 and 3.7.3), a signal for catechol remains throughout the reaction at pH 5 and 8, though this signal gradually becomes less defined. Conversely, for hydroquinone reactions, the signal for the original molecule is only present at the early stages of the reaction (Figures 3.7.4 and 3.7.5). This finding may show that at least some of the original aromatic structure of catechol is retained in the products, while the same cannot be said for hydroquinone. Appearance of a second singlet at 6.81 ppm in the 1 minute spectrum of birnessite-hydroquinone reaction at pH 5 (Figure 3.7.4) could be evidence of the formation of the p-benzoquinone product. Broadening of the hydroquinone peak in the 1 minute spectrum for birnessite-hydroquinone at pH 8 may provide further evidence of the polymerization observed in UV-vis and supported by the FTIR spectrum (persistence of band near 1600 cm^{-1}) (Kögel-Knabner, 1997; Simpson et al., 2001). It is unclear why this peak does not persist in this case, but may be related to the precipitation of the polymeric species formed.

Several aspects of the spectra strongly support the formation of aliphatic degradation products that are the result of ring cleavage. Previous studies have reported cleavage of the aromatic ring during oxidation (Liu et al., 2011; Majcher et al., 2000; Pillar-Little et al., 2014; Wang and Huang, 1992), and this is a requisite step in the formation of CO_2 during the reactions. A group of three signals which occur as two quartets and one multiplet near 3.5 ppm have been attributed to glycerol (Lu et al., 2018). Cleavage and subsequent hydroxylation occurs to form this product, which seems more prevalent in hydroquinone reactions. This finding may indicate participation of hydroxyl and molecular O_2/O_3 species during the oxidation, as previously

suggested (Larson and Hufnal Jr., 1980; McBride, 1989; Pillar-Little et al., 2014; Remucal et al., 2020). A singlet near 8.4 ppm is characteristic of formate. Additionally, strong signals near 1.9 ppm suggest formation of acetate, which exhibits a singlet at this location. Lastly, the occurrence of peaks at around 5.98 and 7.5 may be indicative of cis,cis-muconic acid, a product that has also been proposed to form during catechol oxidation by ozone (Pillar-Little et al., 2014). Other features exist that have not been positively identified. These include potential aromatic hydrogens which give rise to peaks near 7.4 and 7.6 ppm, and another carboxylic acid that appears near 2.19 ppm. Aside from these compounds, the formation of aliphatic hydrocarbon molecules is suggested by strong signals between 0.7–1.2 ppm. Particularly, a doublet at 0.8 ppm and a singlet at 1.16 ppm occur consistently in our spectra and may indicate the presence of methyl and methylene groups. However, a chemical formula cannot be proposed based on this information alone. The identification of carboxylic acids aligns well with the findings of our FTIR study.

3.8 **Mineral phase transformation: XRD**

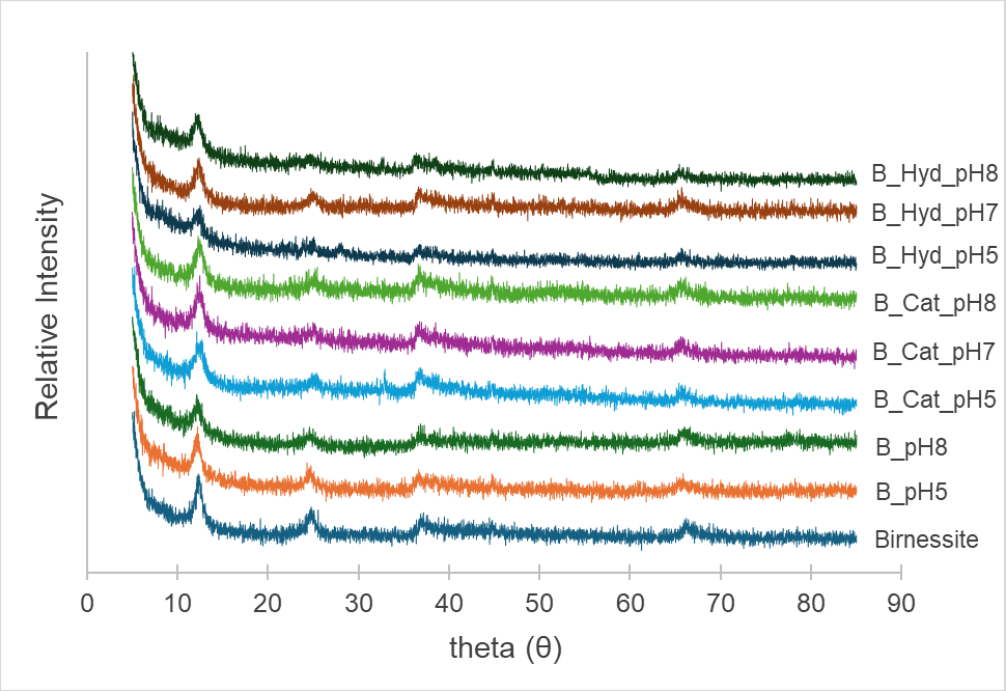

Figure 3.8.1. XRD patterns of birnessite before and after reacting with catechol or hydroquinone at different pH conditions.

The synthetic birnessite in this study has four characteristic peaks in the XRD pattern, corresponding to the (001), (002), (100), and (110) planes in hexagonal birnessite minerals (Drits et al., 1997). No significant changes in the mineral structures show in the XRD patterns of birnessite after reacting with catechol or hydroquinone (Figure 3.8.1). Though a characteristic peak of $MnCO_3$ shows up in the above FTIR results of some mineral samples, no corresponding peaks appear in XRD patterns. This may be ascribed to a very low amount of $MnCO_3$ formed or the poor crystallinity of the newly formed Mn-phases that cannot be detected by XRD.

Altogether, catechol and hydroquinone reduce a fraction of Mn in birnessite while being oxidized. However, there is not significant phase transformation of birnessite at the studied OC:Mn molar ratio. Therefore, the remaining birnessite mineral still has plenty of capability to oxidize more organic compounds at a higher OC:Mn ratio.

SECTION 4: CONCLUSIONS

In this study, the reactions of catechol and hydroquinone with birnessite have been compared across the range of common soil pH conditions to provide an improved understanding of fundamental mechanisms that regulate the fate of simple organic compounds. Spectroscopic analyses were employed to complement direct measurements of Mn dissolution, dissolved organic carbon (DOC), and OC sorption. Molecular structure and pH were both found to have major impacts on the reaction progress. Absence of oxygen did not hinder the oxidation of organic compounds by birnessite.

Catechol was capable of producing more Mn^{2+} through reductive dissolution, and this was greater at low pH. The observed pH effect is related to the deprotonation of birnessite edge sites (PZC 6-8) (Wang et al., 2018). These sites are expected to be the preferred reaction sites because vacant sites will have a greater negative charge (PZC 2-3) and will repel the electron density of the organic molecule (Balgooyen et al., 2020). Along with this finding were greater DOC losses of catechol than hydroquinone; this may suggest that catechol is more susceptible to degradation and loss as CO_2. Sorption of OC to birnessite was greater for catechol and encouraged by low pH conditions. The combination of these findings shows that the ortho position of hydroxyl functional groups enabled catechol to be more reactive compared with the para conformation of hydroquinone. Since mineral association is an important stabilization route for soil organic carbon (Kleber et al., 2015), these results would suggest that the greatest opportunity for sequestration of soil carbon would occur when catechol reacts at low pH. The fact that more DOC remained in solution during hydroquinone reactions provides no guarantee that this carbon would be more stabilized, since it also did not become associated with the

birnessite surface. Considering this, the oxidized molecules would still be susceptible to microbial degradation under natural soil conditions.

Results of UV-vis spectroscopy showed that both compounds reacted to form the respective benzoquinone product, as predicted by the reaction mechanism. Conversion to an oxidized product was rapid and complete for both compounds. Overall, high pH conditions encouraged the formation of polymeric products, since this was observed for both compounds at pH 8. Based on our findings, hydroquinone appears to require high pH conditions to engage in coupling reactions when the OC:birnessite ratio is low. When catechol reacts at low pH, o-benzoquinone was found to be an intermediate in the formation of the polymerized species, and it is not clear if the same can be said for the reaction at high pH. When comparing the compounds, it appears that the ortho position of hydroxyl groups is advantageous in the ability to form polymerized species.

Despite detection of sorbed C, FTIR spectra of the birnessite mineral did not reveal presence of organic functional groups. These findings may differ according to the ratio of OC:birnessite. Formation of a surface complex may be confirmed by the disappearance of a peak near 917 cm^{-1} upon reaction of organic compounds. However, this feature is not always observed in birnessite spectra. The identity of oxidized organic products, as revealed by FTIR spectra of freeze-dried organic residues, did not vary as a function of time. The overall interpretation of the results is most consistent with the formation of a mixture of carboxylic and aromatic functional groups. For reaction conditions where UV-vis results supported the formation of polymers, it appears that the absorption band near or above 1600 cm^{-1} was preserved. Formation of carboxylic functional groups is likely indicated by absorption bands near 1580 and 1380 cm^{-1}. It is unclear if these bands may also be related to the formation of benzoquinones, but seems likely

when comparing hydroquinone spectra across pH conditions. Similar functional groups were observed regardless of oxygen availability.

^{1}NMR spectra supported findings of the production of carboxylic acids upon reaction with birnessite. Cleavage of the aromatic ring appeared to occur for catechol and hydroquinone. Glycerol is a major product formed as a result of cleavage and hydroxylation. This product has not been widely identified previously. Carboxylic acids identified include formate and acetate. Cis,cis-muconic acid may also form, though signals for this compound are relatively weak. New signals for aromatic hydrogens appear in catechol and hydroquinone spectra which have not been positively identified considering the array of potential products to form. For catechol, which appears to partake in polymerization across all pH conditions, the original signal was maintained throughout the duration of the experiment.

A holistic view of the data presented indicates that birnessite is an important mineral for transforming phenolic compounds in soils. These transformations will vary depending on molecular structure and pH, and will occur under oxic and anoxic conditions. As compounds with catecholate functional groups react with birnessite, we can expect that ring cleavage will occur to form carboxylic acids and CO_2. However, oxidative coupling of these aromatic rings also takes place, and at low pH these polymers are readily sorbed to the mineral phase. When hydroquinone reacts, ring cleavage may still occur, with the dominant products being benzoquinone and carboxylic acids. Appreciable polymerization of oxidized products from hydroquinone is only observed at high pH. Under the OC:birnessite ratio studied, the greatest potential for carbon stabilization occurs when catechol reacts at pH 5, in which the products readily sorb to the mineral. Reaction with hydroquinone will be mostly a destabilization process under these conditions. The functional groups studied here are commonly found in the molecular

structures of natural soil organic matter molecules. When these larger molecules react with Mn-oxides, similar trends of stabilization/destabilization may be observed. Many factors will affect the outcome of the reactions presented. Future work could examine the effect of Mn-oxide mineral, the combination of multiple organic compounds, and the ability of these phenols to induce the destabilization of mineral associated carbon.

REFERENCES

Akafia, M.M., Harrington, J.M., Bargar, J.R., Duckworth, O.W., 2014. Metal oxyhydroxide dissolution as promoted by structurally diverse siderophores and oxalate. Geochimica et Cosmochimica Acta 141, 258–269. https://doi.org/10.1016/j.gca.2014.06.024

Aktas, N., Sahiner, N., Kantolu, Ö., Salih, B., Tanyolaç, A., 2003. Biosynthesis and Characterization of Laccase Catalyzed Poly(Catechol). Journal of Polymers and the Environment 11, 123–128. https://doi.org/10.1023/A:1024639231900

Allard, S., Gutierrez, L., Fontaine, C., Croué, J.-P., Gallard, H., 2017. Organic matter interactions with natural manganese oxide and synthetic birnessite. Science of The Total Environment 583, 487–495. https://doi.org/10.1016/j.scitotenv.2017.01.120

Balgooyen, S., Remucal, C.K., Ginder-Vogel, M., 2020. Identifying the mechanisms of cation inhibition of phenol oxidation by acid birnessite. Journal of Environmental Quality 49, 1644–1654. https://doi.org/10.1002/jeq2.20144

Burdon, J., 2001. ARE THE TRADITIONAL CONCEPTS OF THE STRUCTURES OF HUMIC SUBSTANCES REALISTIC? Soil Science 166, 752.

Chang Chien, S.W., Chen, H.L., Wang, M.C., Seshaiah, K., 2009. Oxidative degradation and associated mineralization of catechol, hydroquinone and resorcinol catalyzed by birnessite. Chemosphere 74, 1125–1133. https://doi.org/10.1016/j.chemosphere.2008.10.007

Choe, E., 2020. Roles and action mechanisms of herbs added to the emulsion on its lipid oxidation. Food Science and Biotechnology 29. https://doi.org/10.1007/s10068-020-00800-z

Colarieti, M.L., Toscano, G., Ardi, M.R., Greco Jr., G., 2006. Abiotic oxidation of catechol by soil metal oxides. Journal of Hazardous Materials 134, 161–168. https://doi.org/10.1016/j.jhazmat.2005.10.054

Di Leo, P., Pizzigallo, M.D.R., Ancona, V., Di Benedetto, F., Mesto, E., Schingaro, E., Ventruti, G., 2012. Mechanochemical transformation of an organic ligand on mineral surfaces: The efficiency of birnessite in catechol degradation. Journal of Hazardous Materials 201–202, 148–154. https://doi.org/10.1016/j.jhazmat.2011.11.054

Drits, V.A., Silvester, E., Gorshkov, A.I., Manceau, A., 1997. Structure of synthetic monoclinic Na-rich birnessite and hexagonal birnessite; I, Results from X-ray diffraction and selected-area electron diffraction. American Mineralogist 82, 946–961. https://doi.org/10.2138/am-1997-9-1012

Enguita, F.J., Leitão, A.L., 2013. Hydroquinone: Environmental Pollution, Toxicity, and Microbial Answers. Biomed Res Int 2013, 542168. https://doi.org/10.1155/2013/542168

European Commission. Directorate General for the Environment., 2011. Soil :the hidden part of the climate cycle. Publications Office, LU.

Flaig, W., Beutelspacher, H., Rietz, E., 1975. Chemical Composition and Physical Properties of Humic Substances, in: Gieseking, J.E. (Ed.), Soil Components: Vol. 1: Organic Components. Springer, Berlin, Heidelberg, pp. 1–211. https://doi.org/10.1007/978-3-642-65915-7_1

Gerke, J., 2018. Concepts and Misconceptions of Humic Substances as the Stable Part of Soil Organic Matter: A Review. Agronomy 8, 76. https://doi.org/10.3390/agronomy8050076

Gulley-Stahl, H., Hogan, P.A., Schmidt, W.L., Wall, S.J., Buhrlage, A., Bullen, H.A., 2010. Surface Complexation of Catechol to Metal Oxides: An ATR-FTIR, Adsorption, and

Dissolution Study. Environ. Sci. Technol. 44, 4116–4121. https://doi.org/10.1021/es902040u

Hardie, A., 2008. Pathways of Abiotic Humification as Catalyzed by Mineral Colloids [WWW Document]. URL https://harvest.usask.ca/bitstream/handle/10388/etd-08192008-094240/Hardie_a.pdf;jsessionid=09DB13E2A5D3079B5EC9354A6F23A70F?sequence=1 (accessed 6.20.23).

Harrington, J.M., Bargar, J.R., Jarzecki, A.A., Roberts, J.G., Sombers, L.A., Duckworth, O.W., 2012. Trace metal complexation by the triscatecholate siderophore protochelin: structure and stability. Biometals 25, 393–412. https://doi.org/10.1007/s10534-011-9513-7

Hayes, M.H.B., Swift, R.S., 2020. Chapter One - Vindication of humic substances as a key component of organic matter in soil and water, in: Sparks, D.L. (Ed.), Advances in Agronomy. Academic Press, pp. 1–37. https://doi.org/10.1016/bs.agron.2020.05.001

Ito, S., Sugumaran, M., Wakamatsu, K., 2020. Chemical Reactivities of ortho-Quinones Produced in Living Organisms: Fate of Quinonoid Products Formed by Tyrosinase and Phenoloxidase Action on Phenols and Catechols. Int J Mol Sci 21, 6080. https://doi.org/10.3390/ijms21176080

Johnson, K., Purvis, G., Lopez-Capel, E., Peacock, C., Gray, N., Wagner, T., März, C., Bowen, L., Ojeda, J., Finlay, N., Robertson, S., Worrall, F., Greenwell, C., 2015. Towards a mechanistic understanding of carbon stabilization in manganese oxides. Nat Commun 6, 7628. https://doi.org/10.1038/ncomms8628

Jokic, A., Wang, M.C., Liu, C., Frenkel, A.I., Huang, P.M., 2004. Integration of the polyphenol and Maillard reactions into a unified abiotic pathway for humification in nature: the role of δ-MnO2. Organic Geochemistry 35, 747–762. https://doi.org/10.1016/j.orggeochem.2004.01.021

Kleber, M., Eusterhues, K., Keiluweit, M., Mikutta, C., Mikutta, R., Nico, P.S., 2015. Chapter One - Mineral–Organic Associations: Formation, Properties, and Relevance in Soil Environments, in: Sparks, D.L. (Ed.), Advances in Agronomy. Academic Press, pp. 1–140. https://doi.org/10.1016/bs.agron.2014.10.005

Kögel-Knabner, I., 1997. 13C and 15N NMR spectroscopy as a tool in soil organic matter studies. Geoderma, NMR in Soil Science 80, 243–270. https://doi.org/10.1016/S0016-7061(97)00055-4

Koppenol, W. h., 1982. The reduction potential of the couple O3/O·− 3. FEBS Letters 140, 169–172. https://doi.org/10.1016/0014-5793(82)80886-7

Kubinyi, M.J., Keresztury, G., 1997. Infrared and Raman Spectra of Hydroquinone Crystalline Modifications, in: Mink, J., Keresztury, G., Kellner, R. (Eds.), Progress in Fourier Transform Spectroscopy. Springer, Vienna, pp. 525–528. https://doi.org/10.1007/978-3-7091-6840-0_129

Larson, R.A., Hufnal Jr., J.M., 1980. Oxidative polymerization of dissolved phenols by soluble and insoluble inorganic species1. Limnology and Oceanography 25, 505–512. https://doi.org/10.4319/lo.1980.25.3.0505

Lehmann, J., Kleber, M., 2015. The contentious nature of soil organic matter. Nature 528, 60–68. https://doi.org/10.1038/nature16069

Li, C., Zhang, B., Ertunc, T., Schaeffer, A., Ji, R., 2012. Birnessite-Induced Binding of Phenolic Monomers to Soil Humic Substances and Nature of the Bound Residues. Environ. Sci. Technol. 46, 8843–8850. https://doi.org/10.1021/es3018732

Li, F., Yin, H., Zhu, T., Zhuang, W., 2024. Understanding the role of manganese oxides in retaining harmful metals: Insights into oxidation and adsorption mechanisms at microstructure level. Eco-Environment & Health 3, 89–106. https://doi.org/10.1016/j.eehl.2024.01.002

Li, H., Reinhart, B., Moller, S., Herndon, E., 2023. Effects of C/Mn Ratios on the Sorption and Oxidative Degradation of Small Organic Molecules on Mn-Oxides. Environ. Sci. Technol. 57, 741–750. https://doi.org/10.1021/acs.est.2c03633

Li, H., Santos, F., Butler, K., Herndon, E., 2021. A Critical Review on the Multiple Roles of Manganese in Stabilizing and Destabilizing Soil Organic Matter. Environ. Sci. Technol. 55, 12136–12152. https://doi.org/10.1021/acs.est.1c00299

Ling, F.T., Post, J.E., Heaney, P.J., Kubicki, J.D., Santelli, C.M., 2017. Fourier-transform infrared spectroscopy (FTIR) analysis of triclinic and hexagonal birnessites. Spectrochimica Acta Part A: Molecular and Biomolecular Spectroscopy 178, 32–46. https://doi.org/10.1016/j.saa.2017.01.032

Liu, M.-M., Cao, X.-H., Tan, W.-F., Feng, X.-H., Qiu, G.-H., Chen, X.-H., Liu, F., 2011. Structural Controls on the Catalytic Polymerization of Hydroquinone by Birnessites. Clays Clay Miner. 59, 525–537. https://doi.org/10.1346/CCMN.2011.0590510

Majcher, E.H., Chorover, J., Bollag, J.-M., Huang, P. m., 2000. Evolution of CO2 during Birnessite-Induced Oxidation of 14C-Labeled Catechol. Soil Science Society of America Journal 64, 157–163. https://doi.org/10.2136/sssaj2000.641157x

Matocha, C.J., Sparks, D.L., Amonette, J.E., Kukkadapu, R.K., 2001. Kinetics and Mechanism of Birnessite Reduction by Catechol. Soil Science Society of America Journal 65, 58–66. https://doi.org/10.2136/sssaj2001.65158x

McBride, M.B., 1989. Oxidation of Dihydroxybenzenes in Aerated Aqueous Suspensions of Birnessite. Clays Clay Miner. 37, 341–347. https://doi.org/10.1346/CCMN.1989.0370407

McBride, M.B., 1987. Adsorption and Oxidation of Phenolic Compounds by Iron and Manganese Oxides. Soil Science Society of America Journal 51, 1466–1472. https://doi.org/10.2136/sssaj1987.03615995005100060012x

Naidja, A., Huang, P.M., Bollag, J.-M., 1998. Comparison of Reaction Products from the Transformation of Catechol Catalyzed by Birnessite or Tyrosinase. Soil Science Society of America Journal 62, 188–195. https://doi.org/10.2136/sssaj1998.03615995006200010025x

Pal, S., Bollag, J.-M., Huang, P.M., 1994. Role of abiotic and biotic catalysts in the transformation of phenolic compounds through oxidative coupling reactions. Soil Biology and Biochemistry 26, 813–820. https://doi.org/10.1016/0038-0717(94)90297-6

Pillar-Little, E.A., Camm, R.C., Guzman, M.I., 2014. Catechol Oxidation by Ozone and Hydroxyl Radicals at the Air–Water Interface. Environ. Sci. Technol. 48, 14352–14360. https://doi.org/10.1021/es504094x

Pillar-Little, E.A., Zhou, R., Guzman, M.I., 2015. Heterogeneous Oxidation of Catechol. J. Phys. Chem. A 119, 10349–10359. https://doi.org/10.1021/acs.jpca.5b07914

Potter, R.M., Rossman, G.R., 1979. The tetravalent manganese oxides: identification, hydration, and structural relationships by infrared spectroscopy. American Mineralogist 64, 1199–1218.

Ramírez, F.J., López Navarrete, J.T., 1993. Normal coordinate and rotational barrier calculations on 1,2-dihydroxybenzene. Vibrational Spectroscopy 4, 321–334. https://doi.org/10.1016/0924-2031(93)80006-2

Remucal, C., Ginder-Vogel, M., 2014. A critical review of the reactivity of manganese oxides with organic contaminants. Environmental science. Processes & impacts 16. https://doi.org/10.1039/c3em00703k

Remucal, C.K., Salhi, E., Walpen, N., Von Gunten, U., 2020. Molecular-Level Transformation of Dissolved Organic Matter during Oxidation by Ozone and Hydroxyl Radical. Environ. Sci. Technol. 54, 10351–10360. https://doi.org/10.1021/acs.est.0c03052

Sánchez-Cortés, S., Francioso, O., García-Ramos, J.V., Ciavatta, C., Gessa, C., 2001. Catechol polymerization in the presence of silver surface. Colloids and Surfaces A: Physicochemical and Engineering Aspects 176, 177–184. https://doi.org/10.1016/S0927-7757(00)00630-0

Schweigert, N., Zehnder, A.J.B., Eggen, R.I.L., 2001. Chemical properties of catechols and their molecular modes of toxic action in cells, from microorganisms to mammals. Environmental Microbiology 3, 81–91. https://doi.org/10.1046/j.1462-2920.2001.00176.x

Selvaraj, S., Rajkumar, P., Kesavan, M., Gunasekaran, S., Kumaresan, S., Rajasekar, R., Renuga Devi, T.S., 2019. Spectroscopic and quantum chemical investigations on structural isomers of dihydroxybenzene. Journal of Molecular Structure 1196, 291–305. https://doi.org/10.1016/j.molstruc.2019.06.075

Shindo, H., Huang, P.M., 1992. Comparison of the influence of Mn(IV) oxide and tyrosinase on the formation of humic substances in the environment. Science of The Total Environment, Advances in Humic Substances Research 117–118, 103–110. https://doi.org/10.1016/0048-9697(92)90078-7

Shindo, H., Huang, P.M., 1984. Catalytic Effects of Manganese (IV), Iron(III), Aluminum, and Silicon Oxides on the Formation of Phenolic Polymers. Soil Science Society of America Journal 48, 927–934. https://doi.org/10.2136/sssaj1984.03615995004800040045x

Shindo, H., Huang, P.M., 1982. Role of Mn(IV) oxide in abiotic formation of humic substances in the environment. Nature 298, 363–365. https://doi.org/10.1038/298363a0

Simpson, A.J., Burdon, J., Graham, C.L., Hayes, M.H.B., Spencer, N., Kingery, W.L., 2001. Interpretation of heteronuclear and multidimensional NMR spectroscopy of humic substances. European Journal of Soil Science 52, 495–509. https://doi.org/10.1046/j.1365-2389.2001.00402.x

Šmejkalová, D., Conte, P., Piccolo, A., 2007. Structural Characterization of Isomeric Dimers from the Oxidative Oligomerization of Catechol with a Biomimetic Catalyst. Biomacromolecules 8, 737–743. https://doi.org/10.1021/bm060598o

Stevenson, F.J., 1982. Humus chemistry : genesis, composition, reactions. Wiley.

Stone, A.T., 1987. Reductive Dissolution of Manganese(III/Iv) Oxides by Substituted Phenols. Environ. Sci. Technol. 21, 979–988. https://doi.org/10.1021/es50001a011

Stone, A.T., Morgan, J.J., 1984a. Reduction and dissolution of manganese(III) and manganese(IV) oxides by organics. 1. Reaction with hydroquinone. Environ. Sci. Technol. 18, 450–456. https://doi.org/10.1021/es00124a011

Stone, A.T., Morgan, J.J., 1984b. Reduction and dissolution of manganese(III) and manganese(IV) oxides by organics: 2. Survey of the reactivity of organics. Environ. Sci. Technol. 18, 617–624. https://doi.org/10.1021/es00126a010

Swan, G.A., 1974. Structure, Chemistry, and Biosynthesis of the Melanins, in: Andersen, N.H., Brady, St.F., Harris, C.M., Harris, Th.M., Hecker, E., Hindley, K.B., McGregor, D.N., Marshall, J.A., Roberts, J.C., Schmidt, R., Schrauzer, G.N., Swan, G.A., Tamm, Ch., Wagner, H., Winterfeldt, E., Herz, W., Grisebach, H., Kirby, G.W. (Eds.), Fortschritte

Der Chemie Organischer Naturstoffe / Progress in the Chemistry of Organic Natural Products. Springer, Vienna, pp. 521–582. https://doi.org/10.1007/978-3-7091-7094-6_9

Trainer, E.L., Ginder-Vogel, M., Remucal, C.K., 2021. Selective Reactivity and Oxidation of Dissolved Organic Matter by Manganese Oxides. Environ. Sci. Technol. 55, 12084–12094. https://doi.org/10.1021/acs.est.1c03972

Wang, M.C., Huang, P.M., 1992. Significance of Mn(IV) oxide in the abiotic ring cleavage of pyrogallol in natural environments. Science of The Total Environment, Humic Substances 113, 147–157. https://doi.org/10.1016/0048-9697(92)90022-K

Wang, M.C., Huang, P.M., 1989. Pyrogallol Transformations as Catalyzed by Nontronite, Bentonite, and Kaolinite. Clays Clay Miner. 37, 525–531. https://doi.org/10.1346/CCMN.1989.0370604

Wang, M.C., Huang, P.M., 1986. Humic macromolecule Interlayering in nontronite through interaction with phenol monomers. Nature 323, 529–531. https://doi.org/10.1038/323529a0

Wang, Y., Benkaddour, S., Marafatto, F.F., Peña, J., 2018. Diffusion- and pH-Dependent Reactivity of Layer-Type MnO2: Reactions at Particle Edges versus Vacancy Sites. Environ. Sci. Technol. 52, 3476–3485. https://doi.org/10.1021/acs.est.7b05820

Zhang, Y., Liu, X., Lu, X., 2022. Acidity and metal complexation of edge surface of birnessite-type MnO2: Insight from first principles simulations. The Journal of Chemical Physics 157, 224703. https://doi.org/10.1063/5.0125682

Zhao, W., Liu, F., Feng, X., Tan, W., Qiu, G., Chen, X., 2012. Fourier transform infrared spectroscopy study of acid birnessites before and after Pb^{2+} adsorption. Clay miner. 47, 191–204. https://doi.org/10.1180/claymin.2012.047.2.04